

# Coulomb Excitation with Stable and Radioactive Beams

---

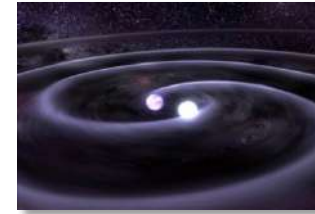
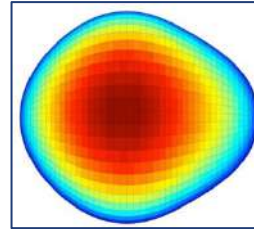
Jack Henderson

University of Warsaw Nuclear Physics Seminar, 10/04/2025

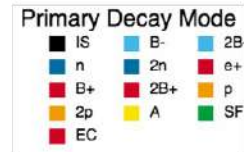
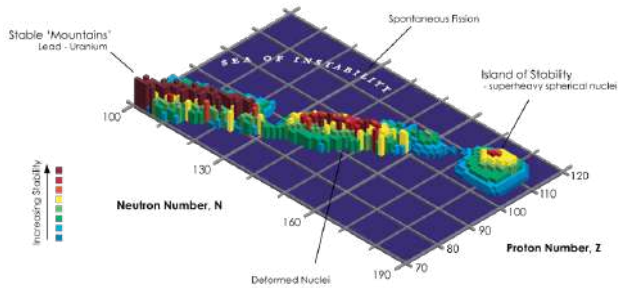


# Why is nuclear physics interesting?

Emergent phenomena in a strongly-interacting many-body system:  
Halo-nuclei, bubble nuclei, collective motion.

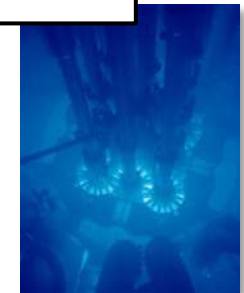


Where are the limits of the nuclear landscape?



Nuclear astrophysics:  
where did the elements  
come from?

Applications:  
Reactor heat, medical  
imaging, etc.



Tests of fundamental physics:  
CKM unitarity, neutrinoless double-  
beta decay, EDM measurements

Nuclear equation of state:  
How heavy can a neutron star be?  
Is there a nuclear superfluid?

## Why is nuclear physics ~~interesting~~ difficult?

The nucleus is a **finite strongly-interacting, many-body** system

# Why is nuclear physics ~~interesting~~ difficult?

The nucleus is a **finite strongly-interacting, many-body** system

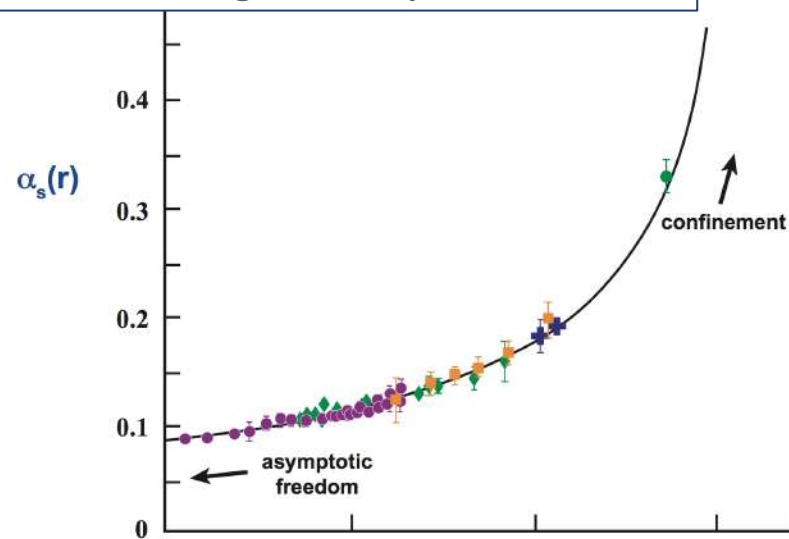
The **finite nature** of the nucleus  
means we can't make trivial use of  
high-N methods from e.g., material  
science

Surface terms matter!

# Why is nuclear physics ~~interesting~~ difficult?

The nucleus is a **finite strongly-interacting, many-body** system

M. R. Pennington, J. Phys G **43** 054001



The **finite nature** of the nucleus means we can't make trivial use of high-N methods from e.g., material science

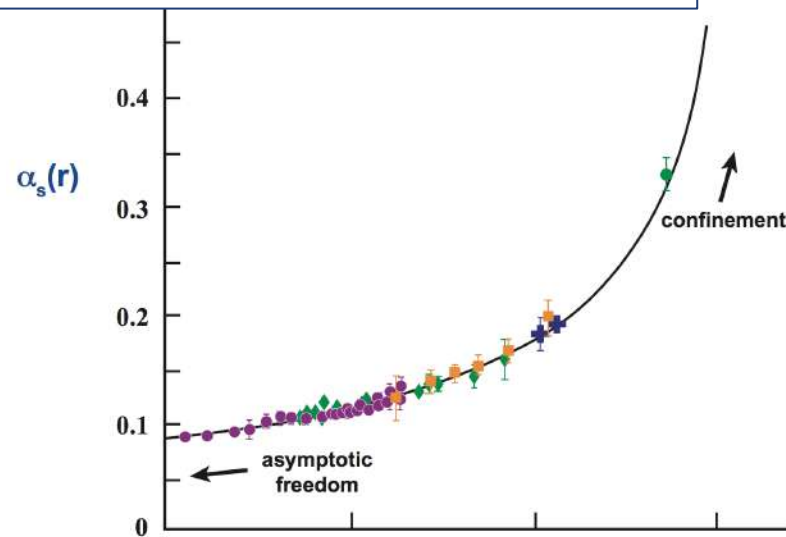
Surface terms matter!

**Strongly interaction is** non-perturbative at low energy (high separation) – cannot trivially neglect low energy (high separation) terms.

# Why is nuclear physics interesting difficult?

The nucleus is a **finite strongly-interacting, many-body** system

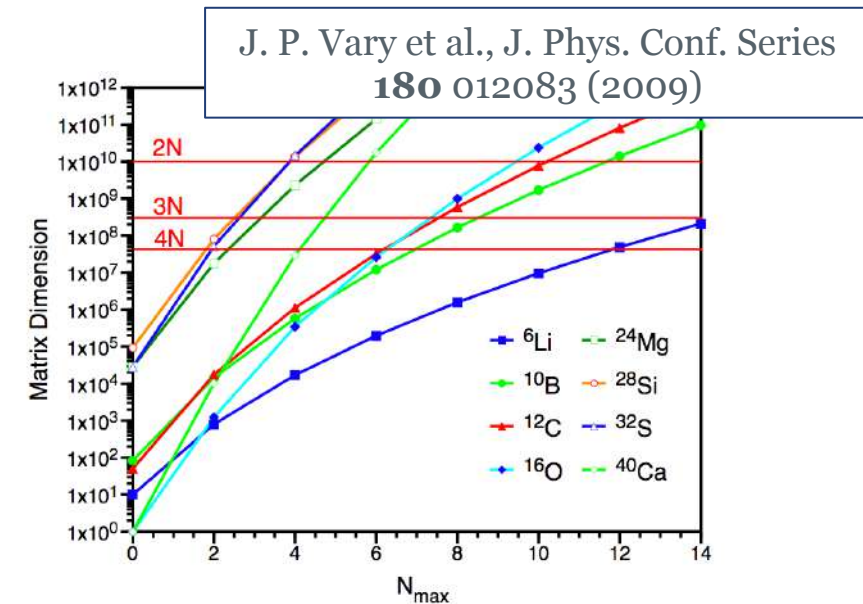
M. R. Pennington, J. Phys G **43** 054001



The **finite nature** of the nucleus means we can't make trivial use of high-N methods from e.g., material science

Surface terms matter!

**Strongly interaction is** non-perturbative at low energy (high separation) – cannot trivially neglect low energy (high separation) terms.



Even with a well understood interaction, solving the **many-body** problem is complicated

Nominally requires diagonalizing the complete highly multi-dimensional Hamiltonian

Rapidly becomes intractable

## Why collectivity?

The nucleus is a **finite strongly-interacting, many-body** system

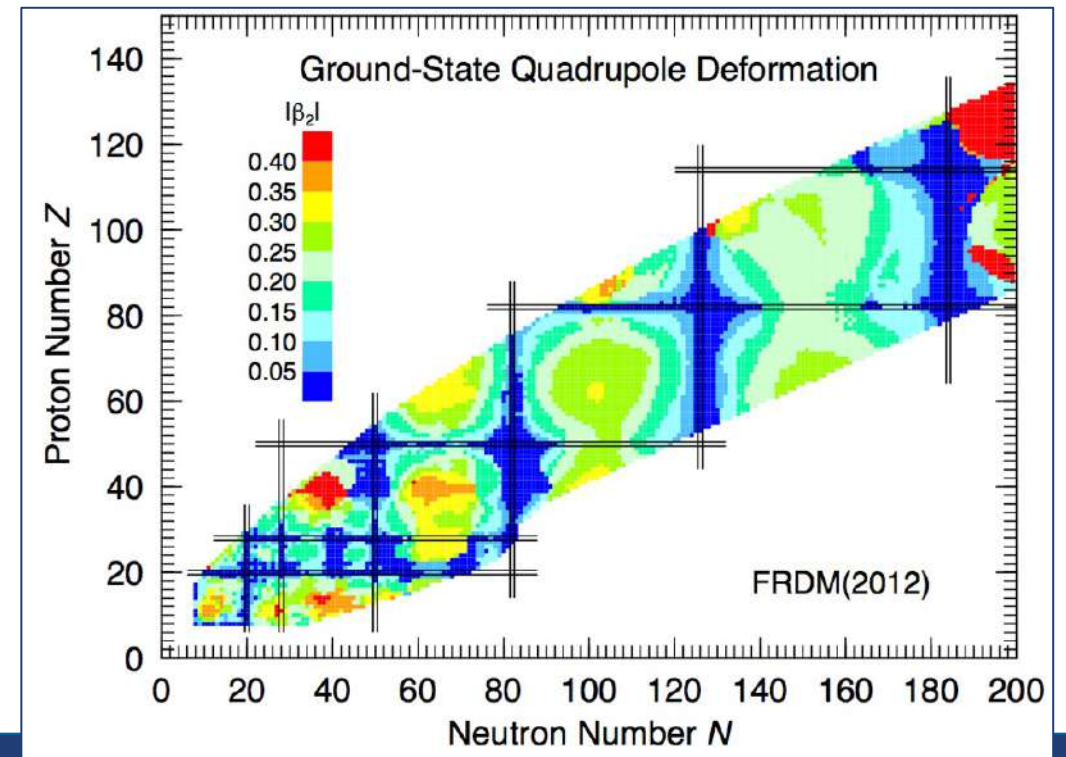
Collective nuclear properties are emergent properties of the nuclear system arising because of the strongly-interacting, many-body nature of the problem

Collectivity (and deformation) is an extreme test of nuclear models

Experimental signature for collectivity is corresponding electric-multipole strength (e.g. E2, E3, E4, etc..)

Inhibited near nuclear magic numbers – but ... everywhere

P. Möller et al., At. Nucl. Data Tables **109** 1 (2016)

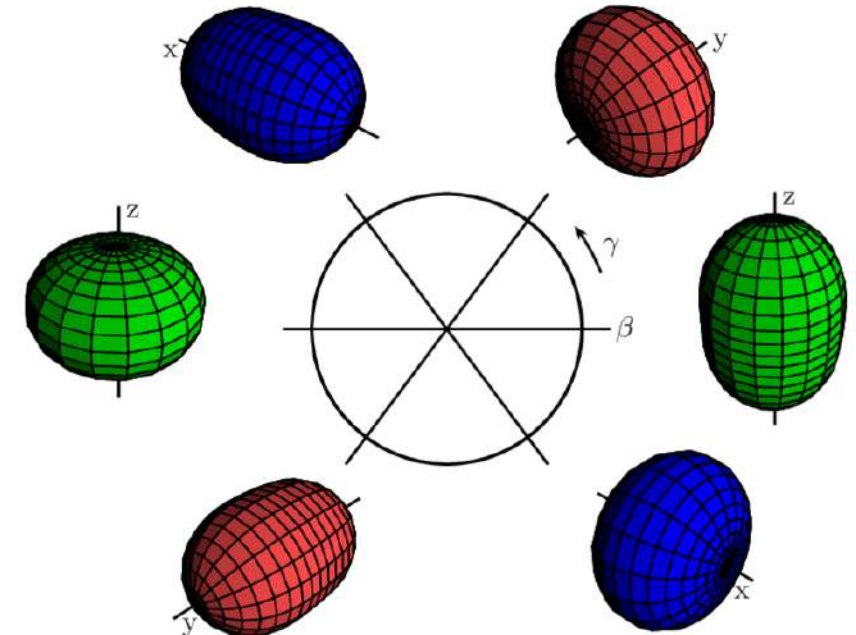
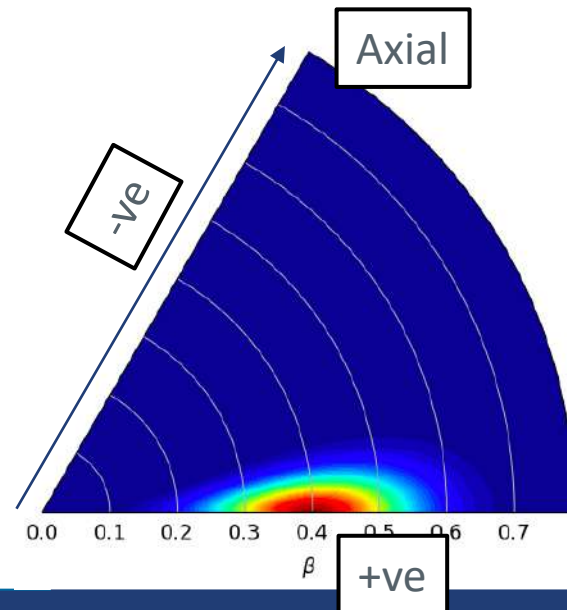
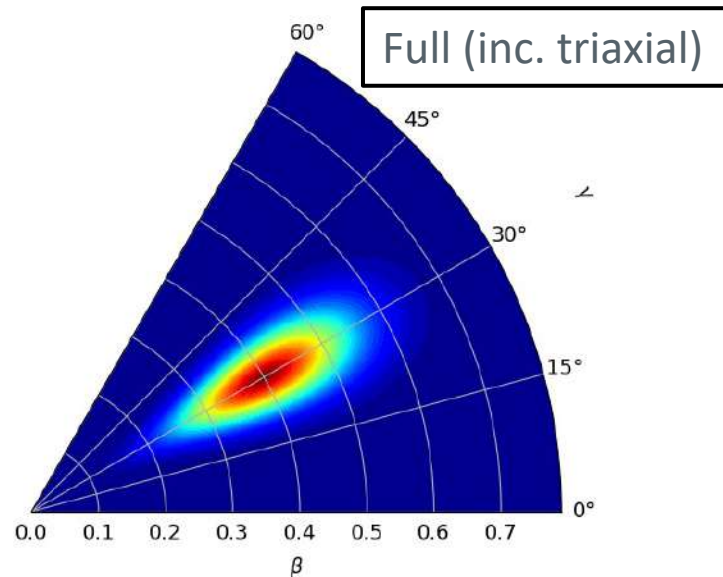


# Language

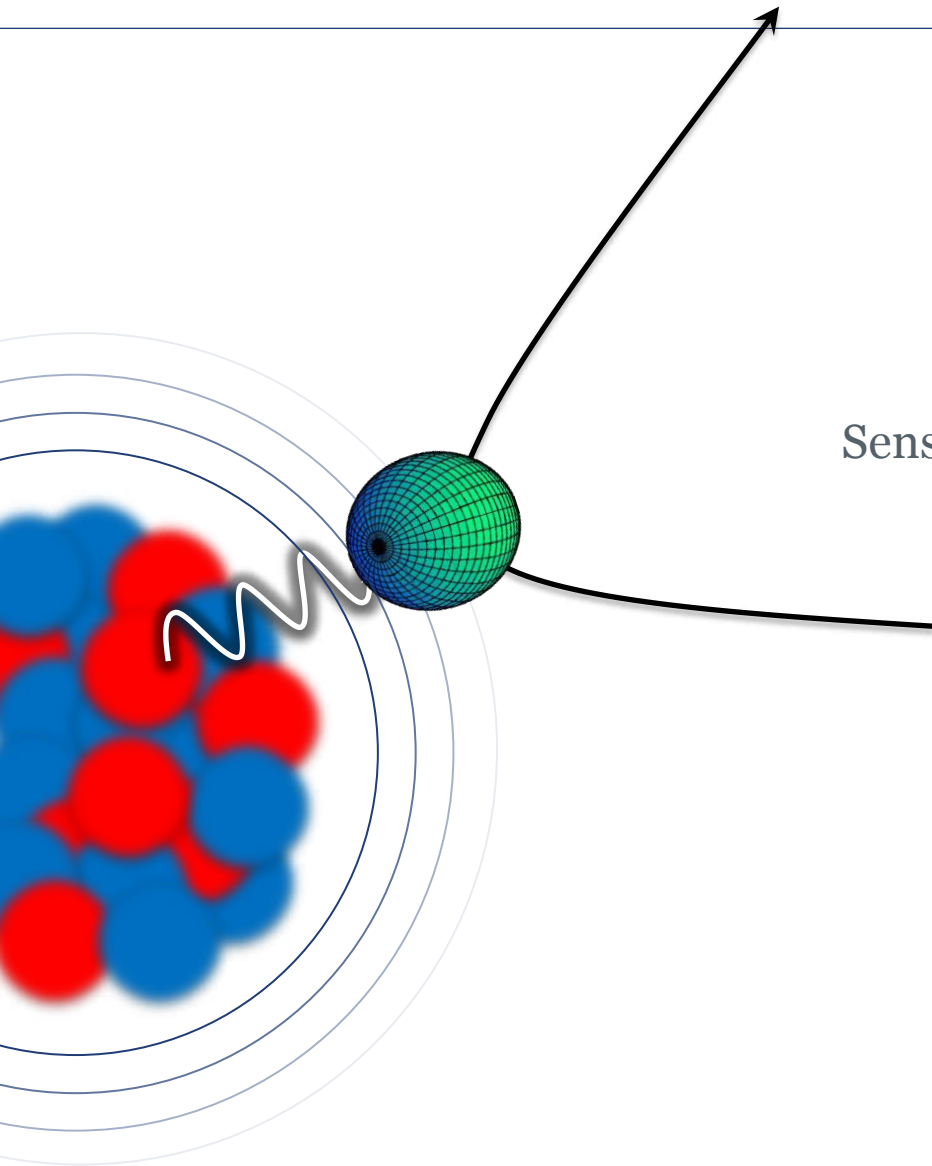
The language of deformation is rooted in the Bohr Hamiltonian, which uses Hill-Wheeler coordinates to relate cartesian axis lengths to  $\beta$  and  $\gamma$  deformation parameters



$$R_k = R_0 \left( 1 + \frac{5}{4\pi} \beta_2 \cos\left(\gamma - \frac{2}{3}\pi k\right) \right)$$



## The Method: Coulomb excitation



### Why Coulomb excitation?

Electromagnetic (“model independent”) probe of the nucleus

Sensitive to magnitudes and (relative) signs of electric multipole matrix elements including spectroscopic quadrupole moments

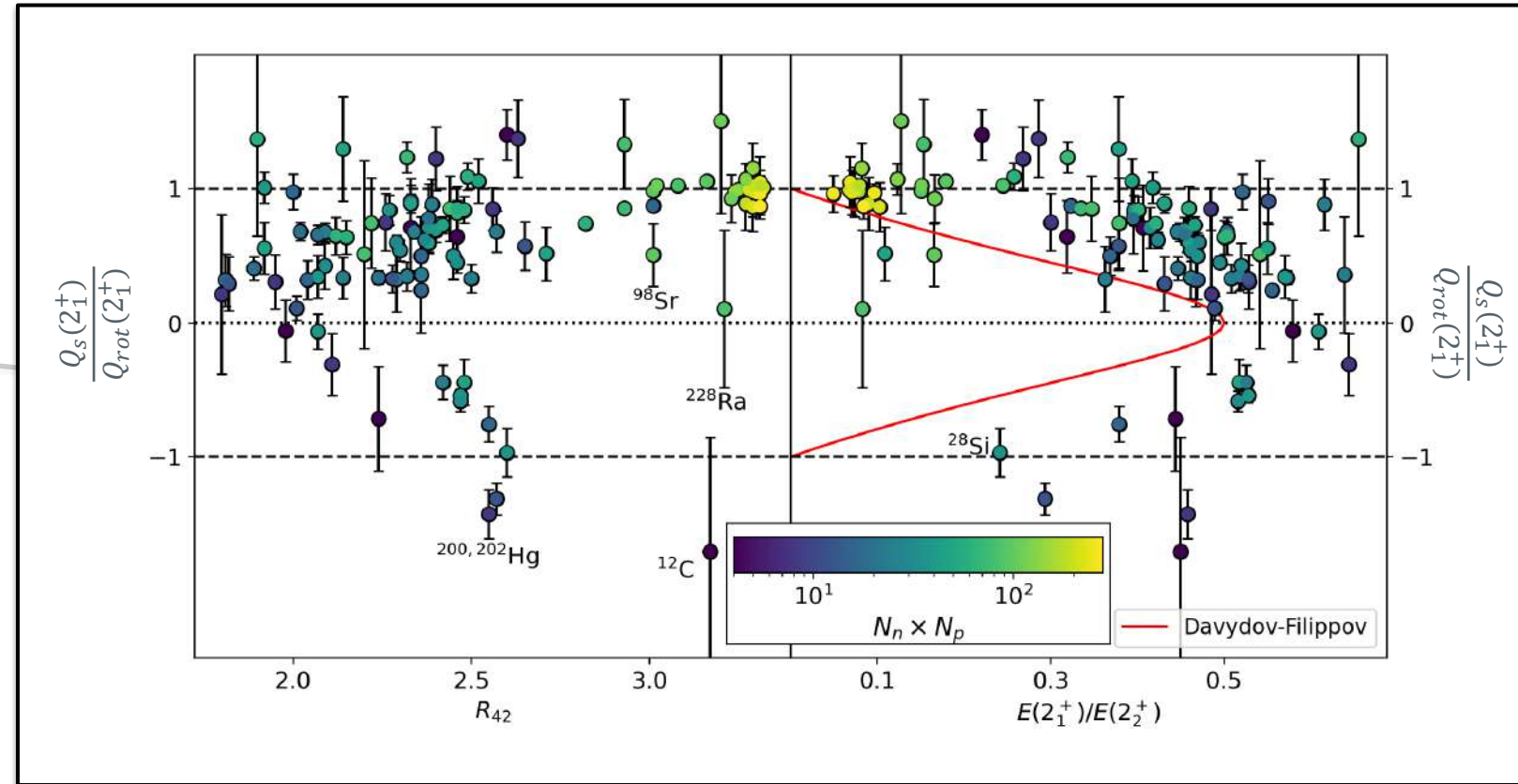
Large cross sections – well-suited to RIB

Exceptional probe of nuclear deformation through sum rules

Kumar PRL **28** 249 (1972)

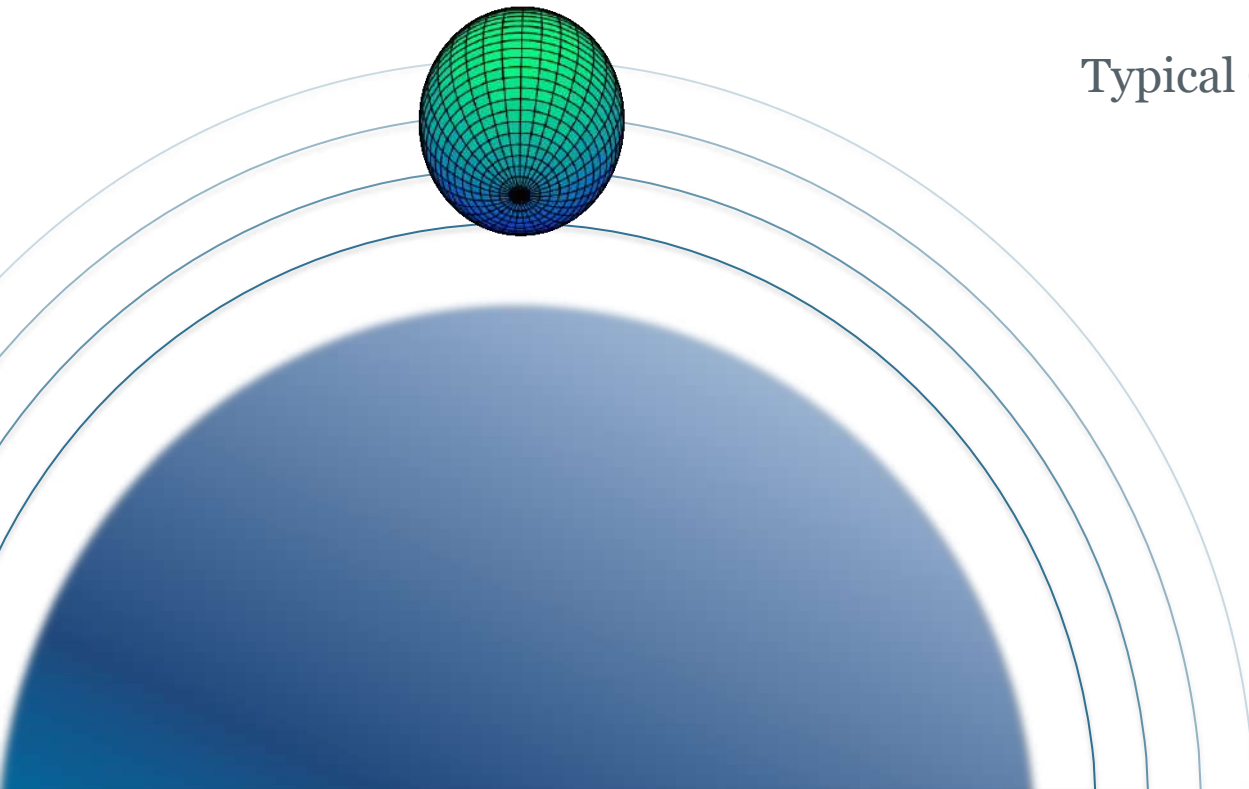
# The Method: Coulomb excitation

Why Coulomb excitation?



## How do we access quadrupole moments?

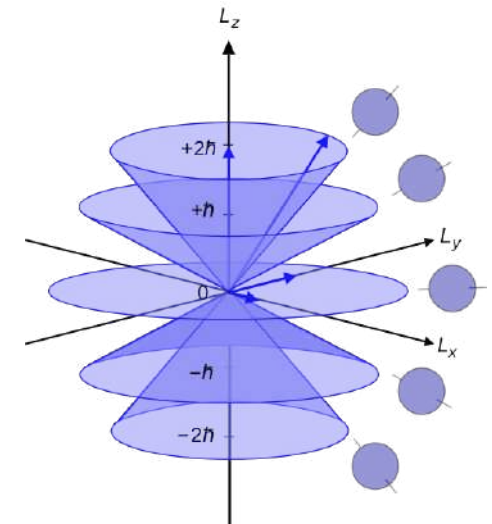
Qualitative picture: Nuclei reorient in electric field gradient to minimize their energy



Typical CoulEx reaction:  $dV/dr \approx 10^{30} \text{ V/cm}^2$

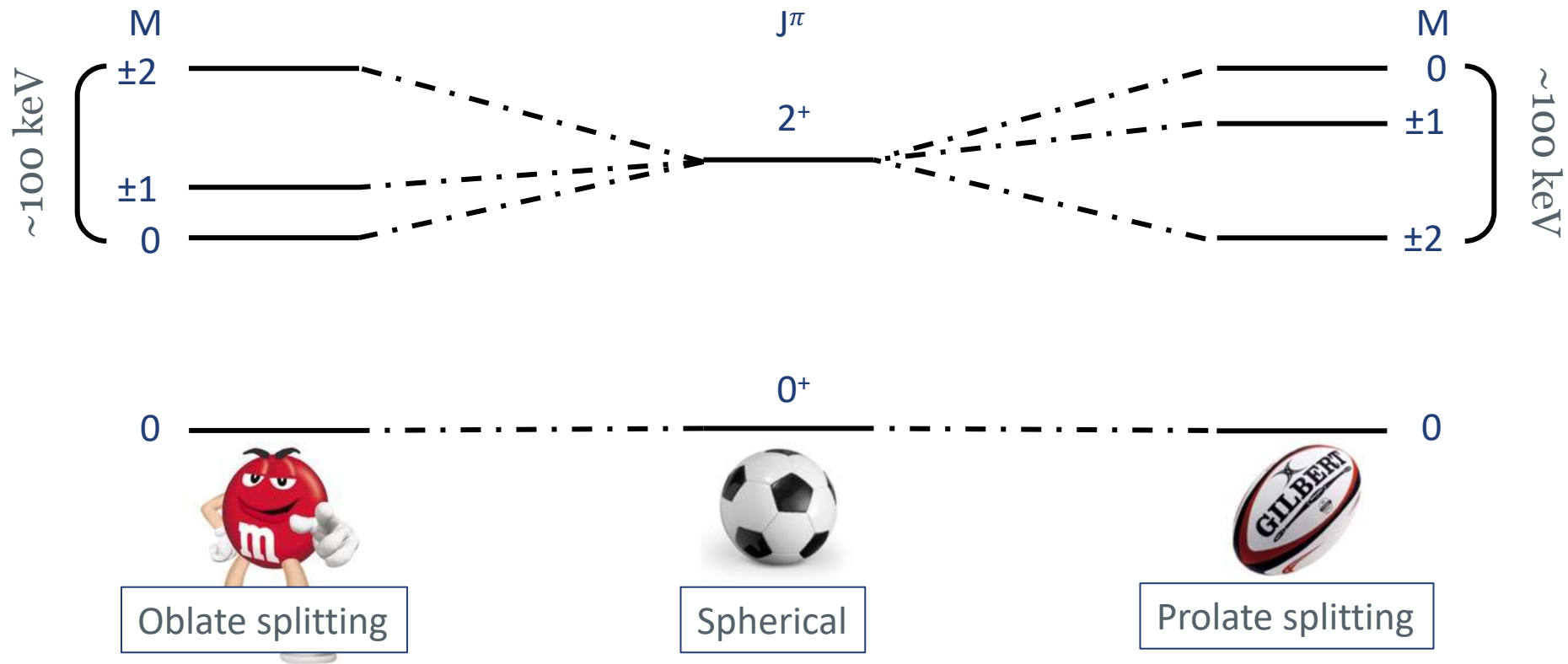
Nucleus aligns relative to symmetry axis

Breaks m-state degeneracy



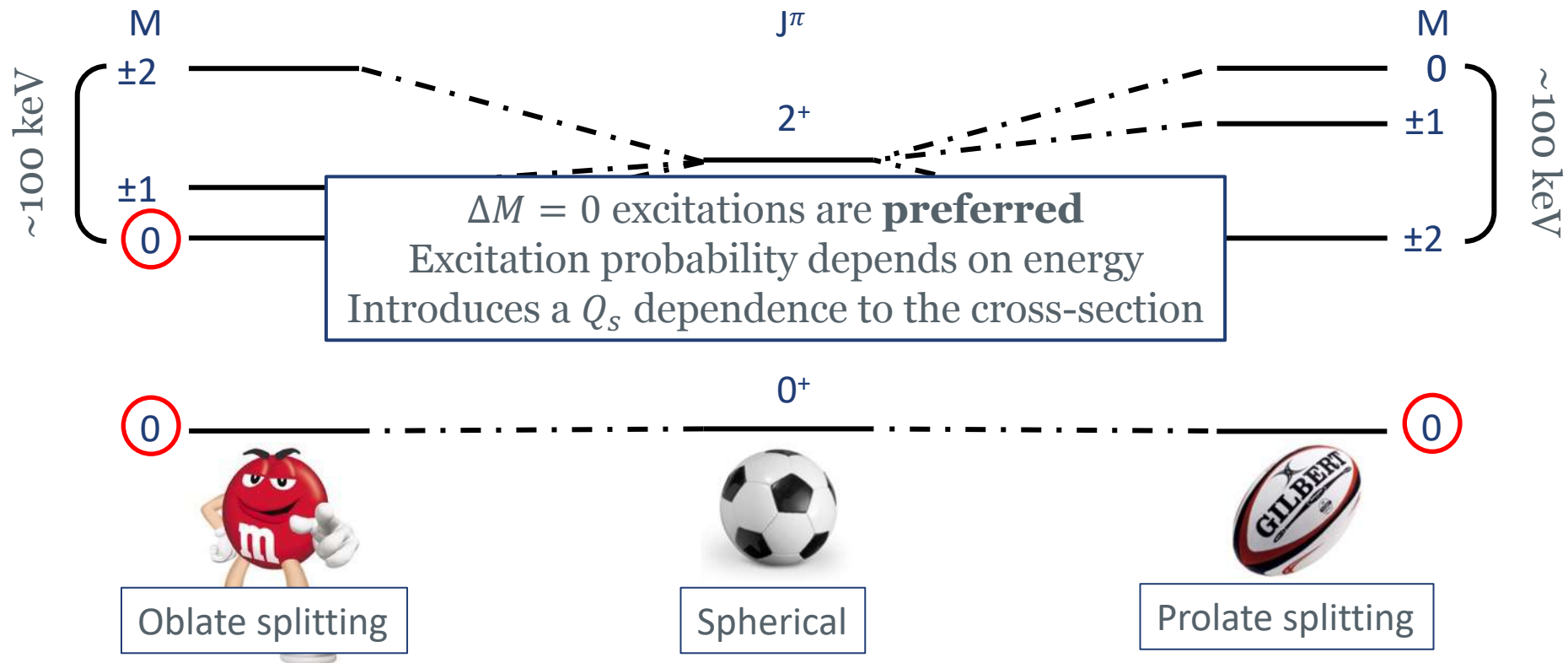
Splitting  $\propto dV/dr \sim 10^{30}$  V/cm

$$E(t) \propto eQ_s Z/r^3(t)$$



Splitting  $\propto dV/dr \sim 10^{30}$  V/cm

$$E(t) \propto eQ_s Z/r^3(t)$$



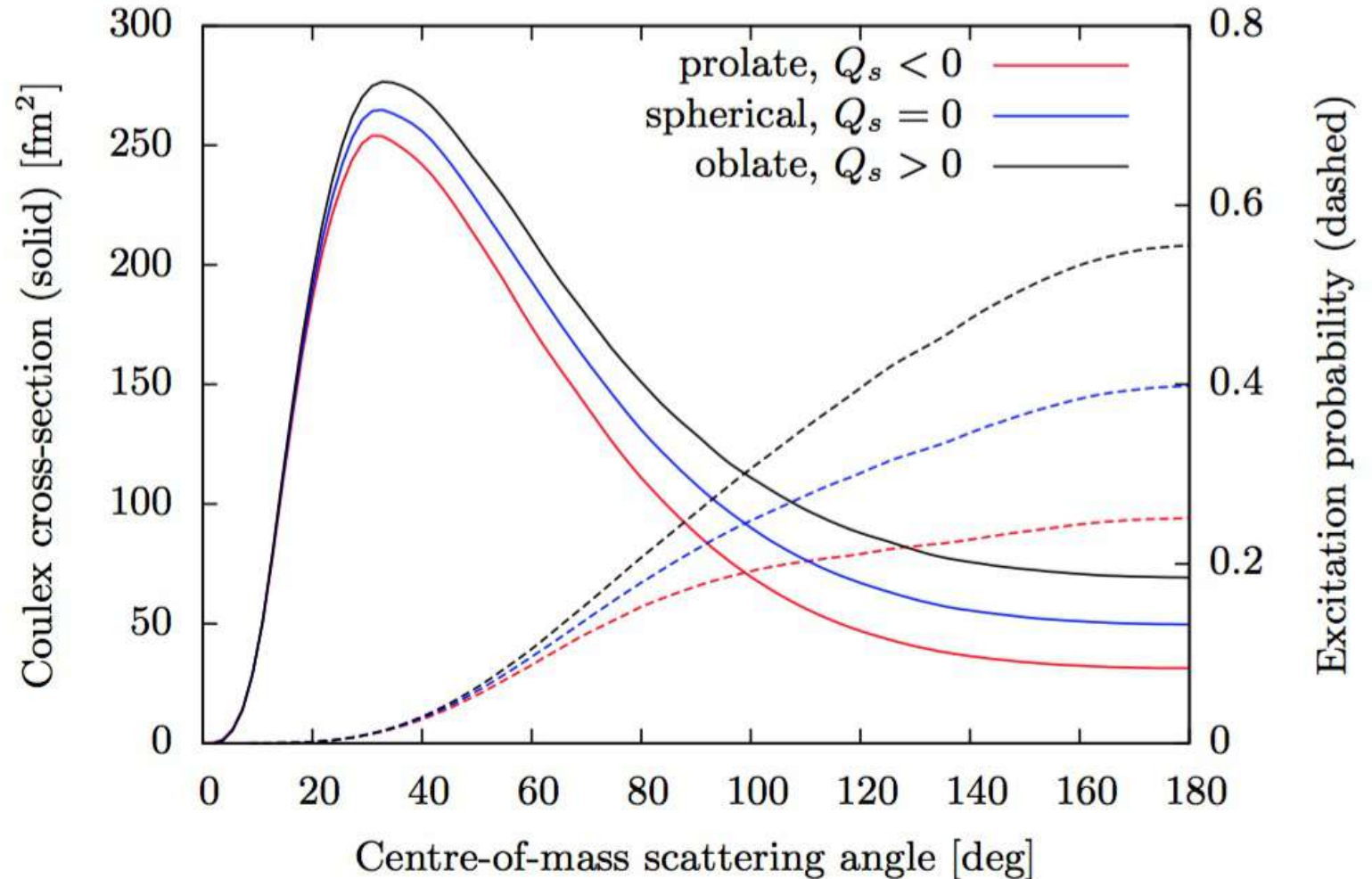
# The Method: Coulomb excitation

Since angle and impact parameter are related, this introduces an additional angular dependence to the cross section

Also influences the angle-integrated cross-section

Measure the distribution and/or the integrated cross-section and access the quadrupole moment

M. Zielinska et al. Eur. J. Phys. A 52 99 (2016)



# The Method: Coulomb excitation

$$\frac{da_k}{d\omega} = -i \sum_{\lambda\mu n} Q_{\lambda\mu}(\epsilon, \omega) \zeta_{kn}^{\lambda\mu} \langle I_k | M(\lambda) | I_n \rangle e^{(i\xi_{kn}(\epsilon \sinh \omega + \omega))} a_n(\omega)$$

a = (sub)state amplitude

$\mu$  = magnetic substate

k = (sub)state being populated

n = (sub)state connected to k

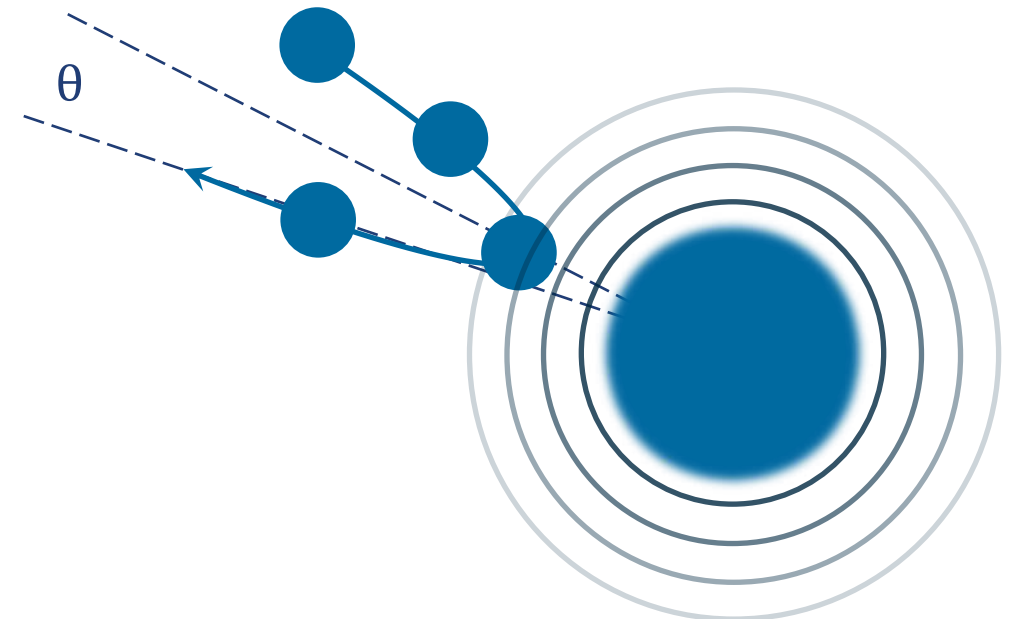
$\lambda$  = multipole

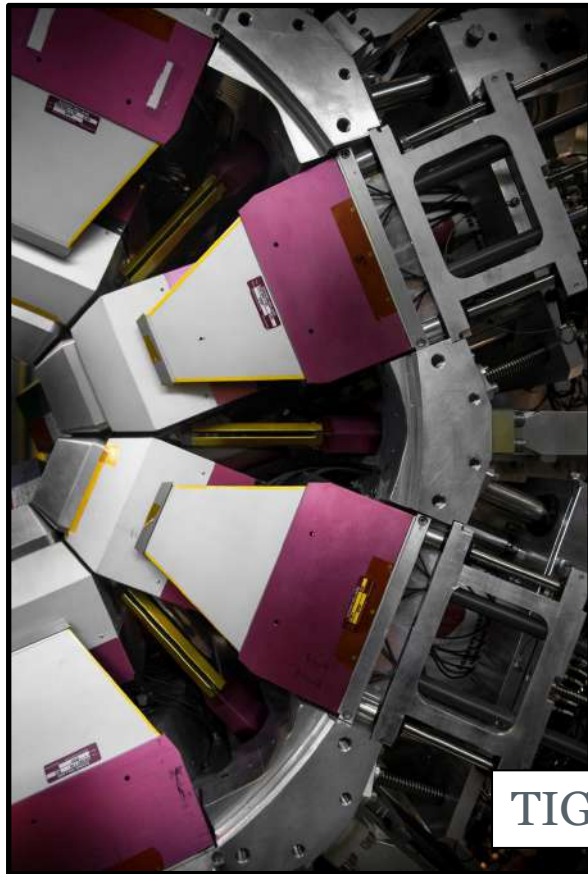
$\langle I_k | M(\lambda) | I_n \rangle$  = electromagnetic matrix element connecting k and n

$Q_{\lambda\mu}(\epsilon, \omega)$  = collision function

$\zeta_{kn}^{\lambda\mu}$  = coupling parameter

$\xi_{kn}$  = adiabaticity parameter

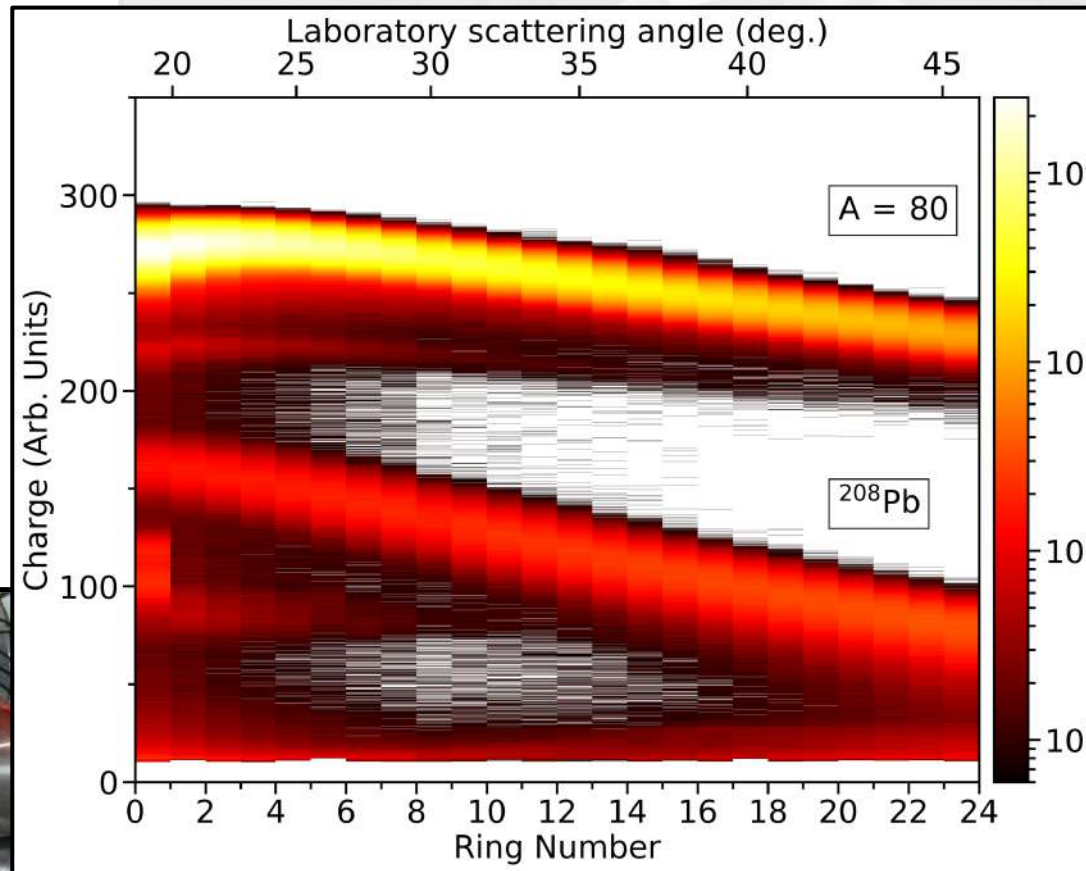
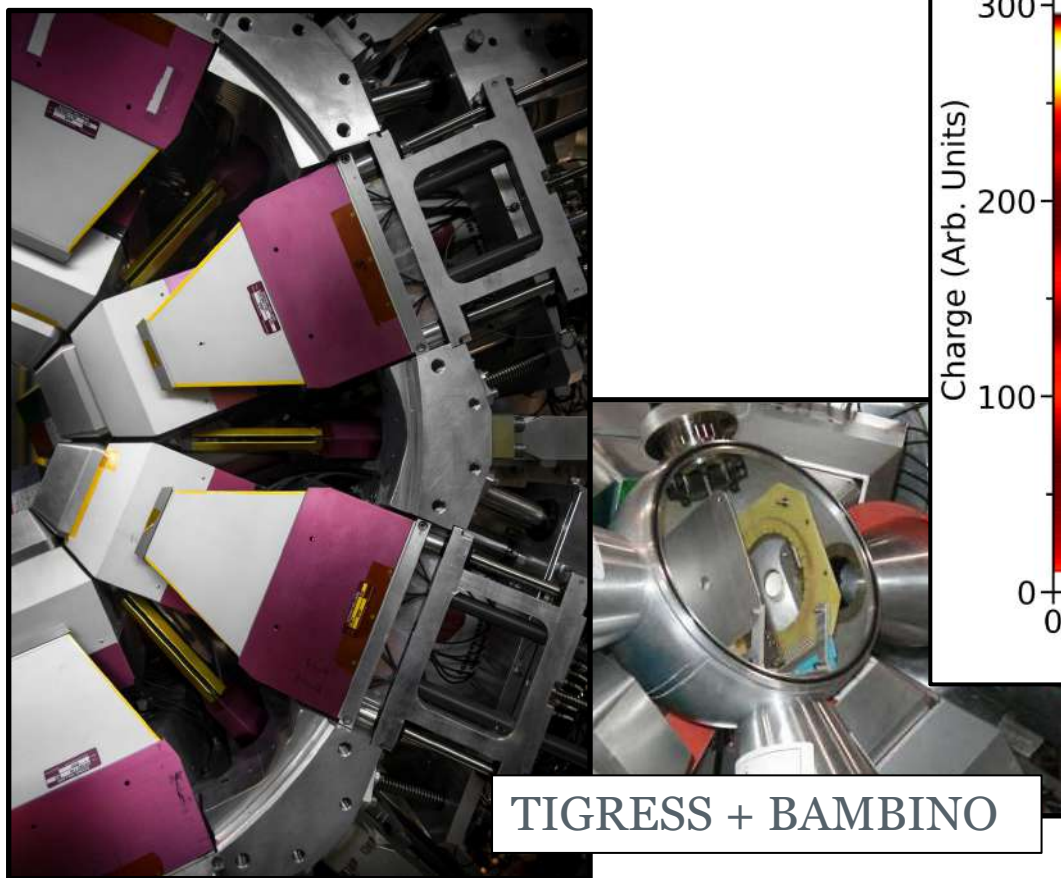




TIGRESS + BAMBINO



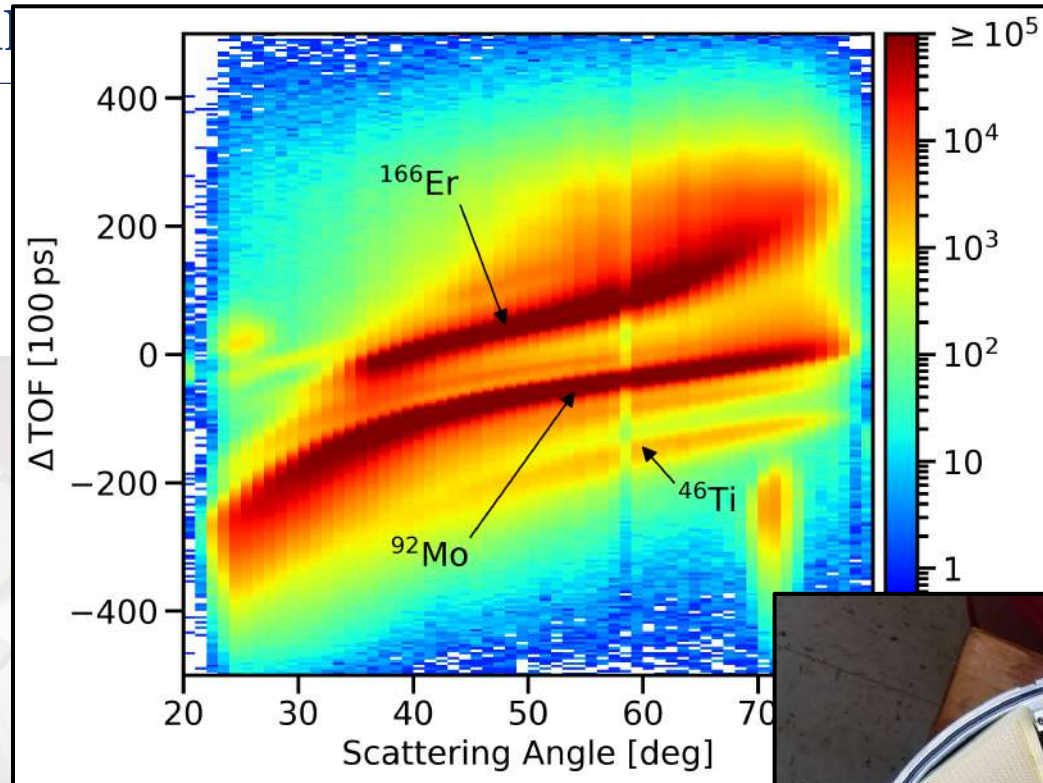
GRETINA + CHICO2



+ CHICO<sub>2</sub>

G. Hackman & C. E. Svensson,  
Hyperfine Interactions **225** 241 (2014)

Result



GREY + CHICO2

S. Paschalis *et al.* NIM A  
**709** 44 (2013)

C. Y. Wu *et al.* NIM A  
**814** 6 (2016)



# Coulomb excitation of $^{208}\text{Pb}$

A quintessential doubly-magic system

Spherical\* ground state

Poves *et al.* PRC **101** 054307 (2020)

First-excited  $3^-$  state, an octupole vibration

D. Goutte *et al.* PRL **45** 1618 (1980)

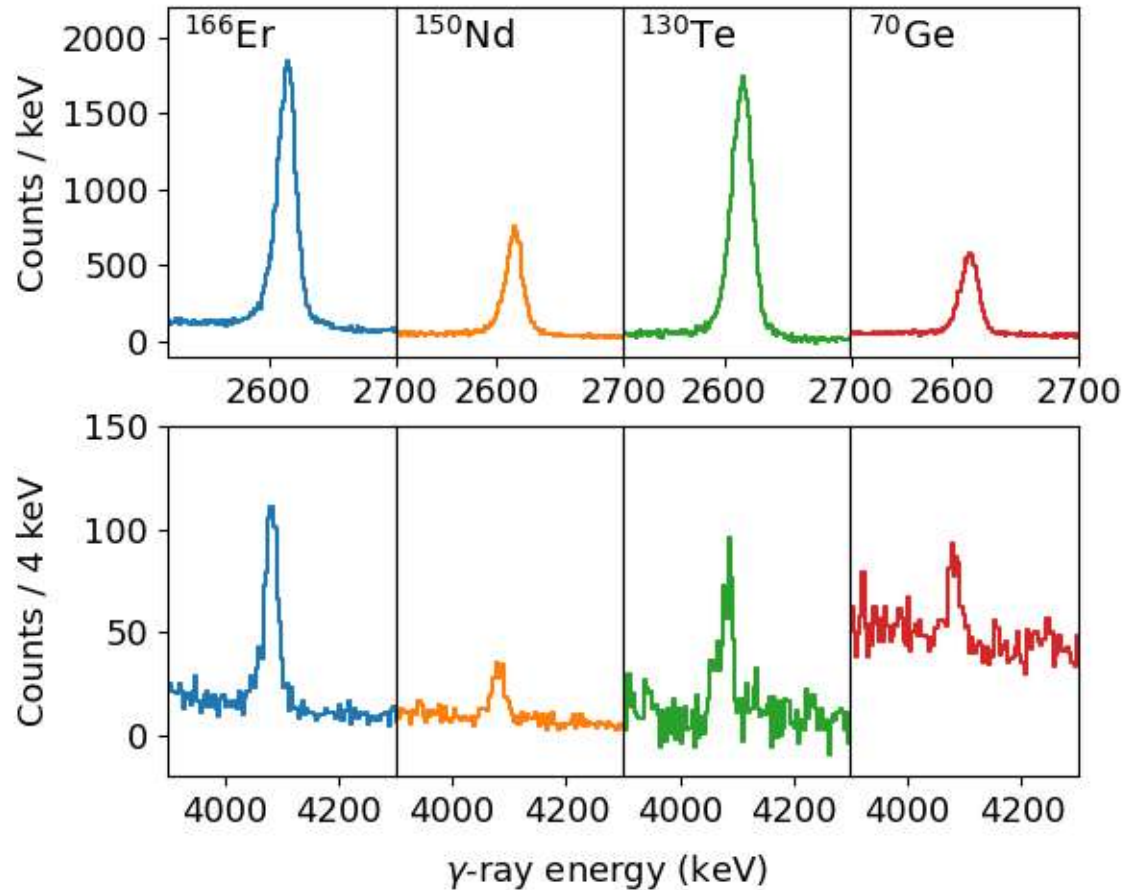
A key benchmark for models and our understanding of EoS through neutron-skin

B. Hu *et al.* Nature Physics **18** 1196 (2022)

D. Adhikari *et al.* PRL **126** 172502 (2021)

Radon Z=86	$^{204}\text{Rn}$ 74.52 s	$^{205}\text{Rn}$ 170 s	$^{206}\text{Rn}$ 5.67 m	$^{207}\text{Rn}$ 9.35 m	$^{208}\text{Rn}$ 24.35 m	$^{209}\text{Rn}$ 26.8 m	$^{210}\text{Rn}$ 144 m	$^{211}\text{Rn}$ 14.6 h	$^{212}\text{Rn}$ 23.9 m	$^{213}\text{Rn}$ 19.5 ms	$^{214}\text{Rn}$ 259 ns	$^{215}\text{Rn}$ 2.3 $\mu\text{s}$	$^{216}\text{Rn}$ 29 $\mu\text{s}$
Astatine Z=85	$^{203}\text{At}$ 7.4 m	$^{204}\text{At}$ 8.12 m	$^{205}\text{At}$ 28.9 m	$^{206}\text{At}$ 30.8 m	$^{207}\text{At}$ 108.5 m	$^{208}\text{At}$ 97.8 m	$^{209}\text{At}$ 5.42 h	$^{210}\text{At}$ 8.1 h	$^{211}\text{At}$ 7.214 h	$^{212}\text{At}$ 314 ms	$^{213}\text{At}$ 125 ns	$^{214}\text{At}$ 558 ns	$^{215}\text{At}$ 37 $\mu\text{s}$
Polonium Z=84	$^{202}\text{Po}$ 44.8 m	$^{203}\text{Po}$ 96.7 m	$^{204}\text{Po}$ 211.14 m	$^{205}\text{Po}$ 104.4 m	$^{206}\text{Po}$ 8.8 d	$^{207}\text{Po}$ 5.9 h	$^{208}\text{Po}$ 2.898 y	$^{209}\text{Po}$ 124 y	$^{210}\text{Po}$ 138.376 d	$^{211}\text{Po}$ 516 ms	$^{212}\text{Po}$ 294.4 ns	$^{213}\text{Po}$ 3.705 $\mu\text{s}$	$^{214}\text{Po}$ 163.47 $\mu\text{s}$
Bismuth Z=83	$^{201}\text{Bi}$ 103 m	$^{202}\text{Bi}$ 101.3 m	$^{203}\text{Bi}$ 11.78 h	$^{204}\text{Bi}$ 11.27 h	$^{205}\text{Bi}$ 14.91 d	$^{206}\text{Bi}$ 8.340 d	$^{207}\text{Bi}$ 31.39 y	$^{208}\text{Bi}$ 368 ky	$^{209}\text{Bi}$ 20.1 Ey	$^{210}\text{Bi}$ 5.012 d	$^{211}\text{Bi}$ 128.4 s	$^{212}\text{Bi}$ 60.55 m	$^{213}\text{Bi}$ 46.6 m
Lead Z=82	$^{200}\text{Pb}$ 21.5 h	$^{201}\text{Pb}$ 8.33 h	$^{202}\text{Pb}$ 32.5 ky	$^{203}\text{Pb}$ 81.364 h	$^{204}\text{Pb}$	$^{205}\text{Pb}$ 11 My	$^{206}\text{Pb}$	$^{207}\text{Pb}$	$^{208}\text{Pb}$	$^{209}\text{Pb}$ 194.1 m	$^{210}\text{Pb}$ 22.2 y	$^{211}\text{Pb}$ 36.1628 m	$^{212}\text{Pb}$ 10.627 h
Thallium Z=81	$^{199}\text{Tl}$ 7.42 h	$^{200}\text{Tl}$ 36.1 h	$^{201}\text{Tl}$ 73.0104 h	$^{202}\text{Tl}$ 12.31 d	$^{203}\text{Tl}$	$^{204}\text{Tl}$ 3.783 y	$^{205}\text{Tl}$	$^{206}\text{Tl}$ 4.202 m	$^{207}\text{Tl}$ 4.77 m	$^{208}\text{Tl}$ 183.18 s	$^{209}\text{Tl}$ 129.72 s	$^{210}\text{Tl}$ 78 s	$^{211}\text{Tl}$ 81 s
Mercury Z=80	$^{198}\text{Hg}$	$^{199}\text{Hg}$	$^{200}\text{Hg}$	$^{201}\text{Hg}$	$^{202}\text{Hg}$	$^{203}\text{Hg}$ 46.61 d	$^{204}\text{Hg}$	$^{205}\text{Hg}$ 5.14 m	$^{206}\text{Hg}$ 8.32 m	$^{207}\text{Hg}$ 174 s	$^{208}\text{Hg}$ 135 s	$^{209}\text{Hg}$ 6.3 s	$^{210}\text{Hg}$ 64 s
Gold Z=79	$^{197}\text{Au}$	$^{198}\text{Au}$ 64.671360 h	$^{199}\text{Au}$ 75.336 h	$^{200}\text{Au}$ 48.4 m	$^{201}\text{Au}$ 26 m	$^{202}\text{Au}$ 28.4 s	$^{203}\text{Au}$ 60 s	$^{204}\text{Au}$ 36.3 s	$^{205}\text{Au}$ 32 s	$^{206}\text{Au}$ 47 s	$^{207}\text{Au}$ 3 s	$^{208}\text{Au}$ 20 s	$^{209}\text{Au}$ 1000 ms
Platinum Z=78	$^{196}\text{Pt}$	$^{197}\text{Pt}$ 19.8915 h	$^{198}\text{Pt}$	$^{199}\text{Pt}$ 30.8 m	$^{200}\text{Pt}$ 12.6 h	$^{201}\text{Pt}$ 150 s	$^{202}\text{Pt}$ 44 h	$^{203}\text{Pt}$ 22 s	$^{204}\text{Pt}$ 10.3 s	$^{205}\text{Pt}$ 2 s	$^{206}\text{Pt}$ 500 ms	$^{207}\text{Pt}$ 600 ms	$^{208}\text{Pt}$ 220 ms

$\Sigma=18$ Bismuth	$^{186}\text{Bi}$	$^{187}\text{Bi}$	$^{188}\text{Bi}$	$^{189}\text{Bi}$	$^{190}\text{Bi}$	$^{191}\text{Bi}$	$^{192}\text{Bi}$	$^{193}\text{Bi}$	$^{194}\text{Bi}$	$^{195}\text{Bi}$	$^{196}\text{Bi}$	$^{197}\text{Bi}$	$^{198}\text{Bi}$
$\Sigma=19$ Uranium	$^{187}\text{U}$	$^{188}\text{U}$	$^{189}\text{U}$	$^{190}\text{U}$	$^{191}\text{U}$	$^{192}\text{U}$	$^{193}\text{U}$	$^{194}\text{U}$	$^{195}\text{U}$	$^{196}\text{U}$	$^{197}\text{U}$	$^{198}\text{U}$	$^{199}\text{U}$
$\Sigma=80$ Mercury	$^{180}\text{Hg}$	$^{181}\text{Hg}$	$^{182}\text{Hg}$	$^{183}\text{Hg}$	$^{184}\text{Hg}$	$^{185}\text{Hg}$	$^{186}\text{Hg}$	$^{187}\text{Hg}$	$^{188}\text{Hg}$	$^{189}\text{Hg}$	$^{190}\text{Hg}$	$^{191}\text{Hg}$	$^{192}\text{Hg}$



Lead-208 targets often used in Coulomb excitation – clean spectra!

Combine data from four separate Coulomb-excitation measurements:  $^{166}\text{Er}$ ,  $^{150}\text{Nd}$ ,  $^{130}\text{Te}$  and  $^{70}\text{Ge}$

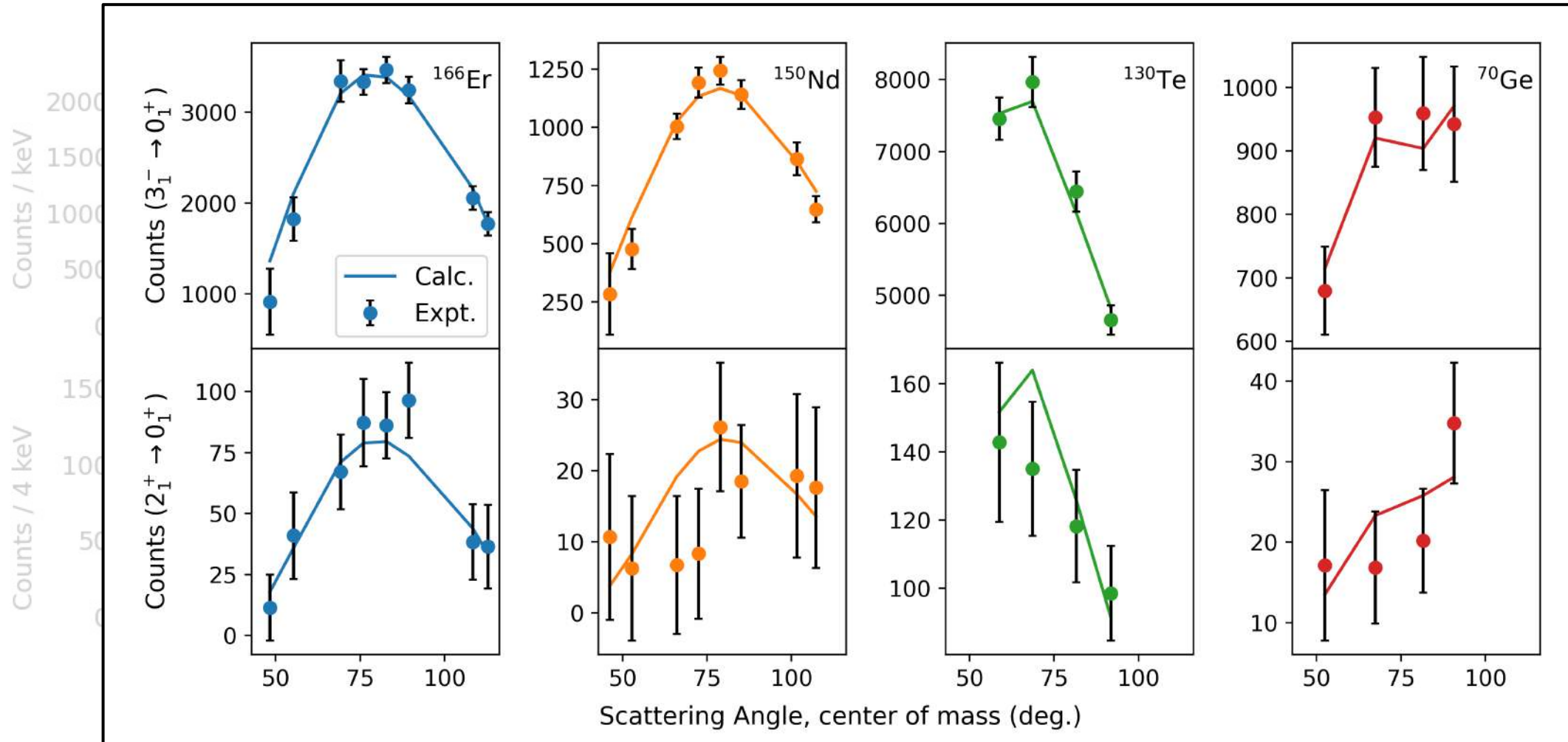
See  $3_1^- \rightarrow 0_1^+$  and  $2_1^+ \rightarrow 0_1^+$  transitions

All data taken with CHICO2 and GRETINA in 2022

Data analysed and matrix elements simultaneously minimised using GOSIA

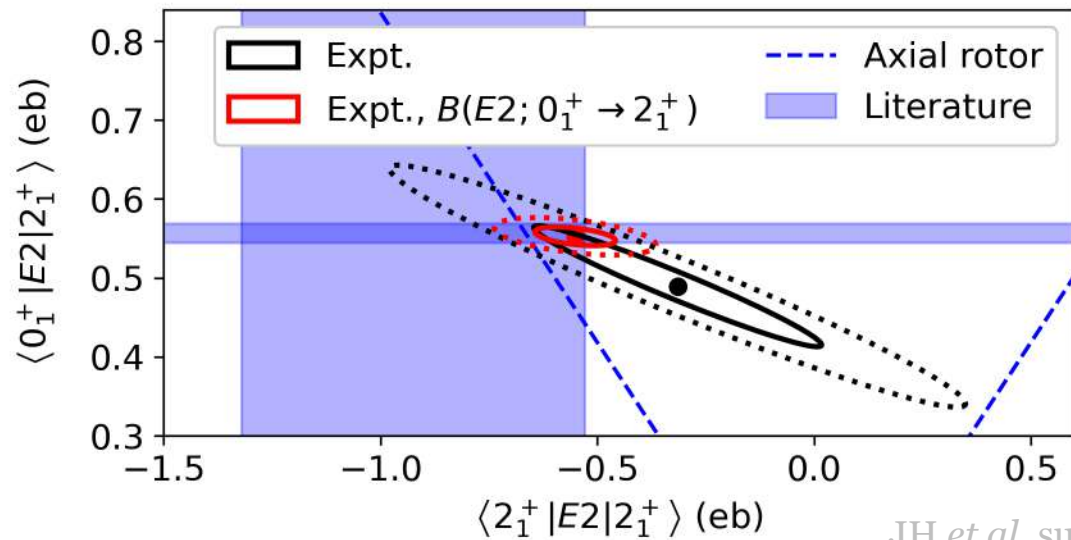
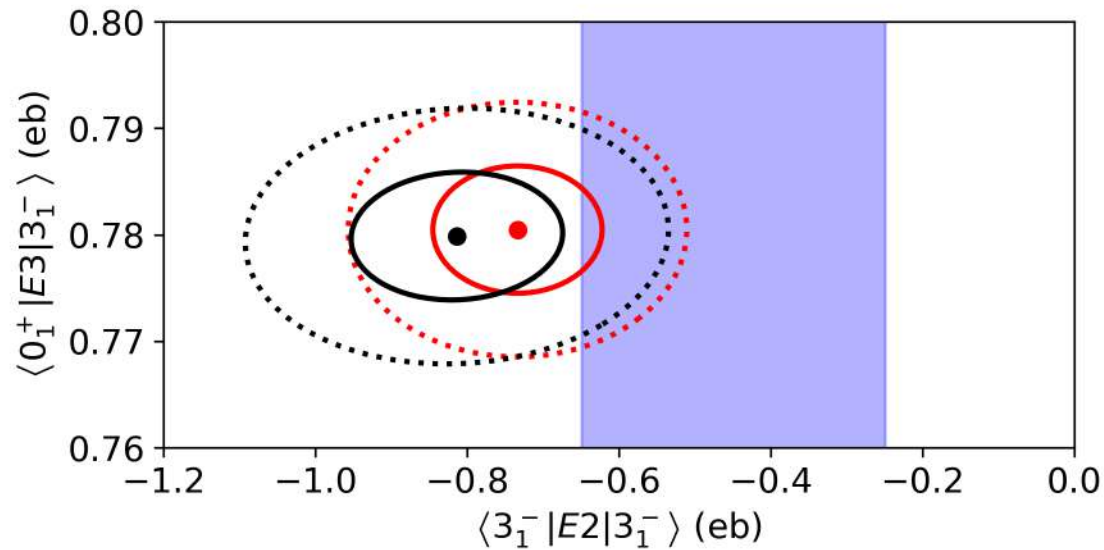
<https://github.com/jhenderson88/GOSIAFitter>

# Coulomb excitation of $^{208}\text{Pb}$



JH *et al.* submitted for publication

# Coulomb excitation of $^{208}\text{Pb}$



Extract  $\langle 0_1^+ | E2 | 2_1^+ \rangle$ ,  $\langle 0_1^+ | E3 | 3_1^- \rangle$ ,  $\langle 2_1^+ | E2 | 2_1^+ \rangle$  and  $\langle 3_1^- | E2 | 3_1^- \rangle$  matrix elements and their correlations

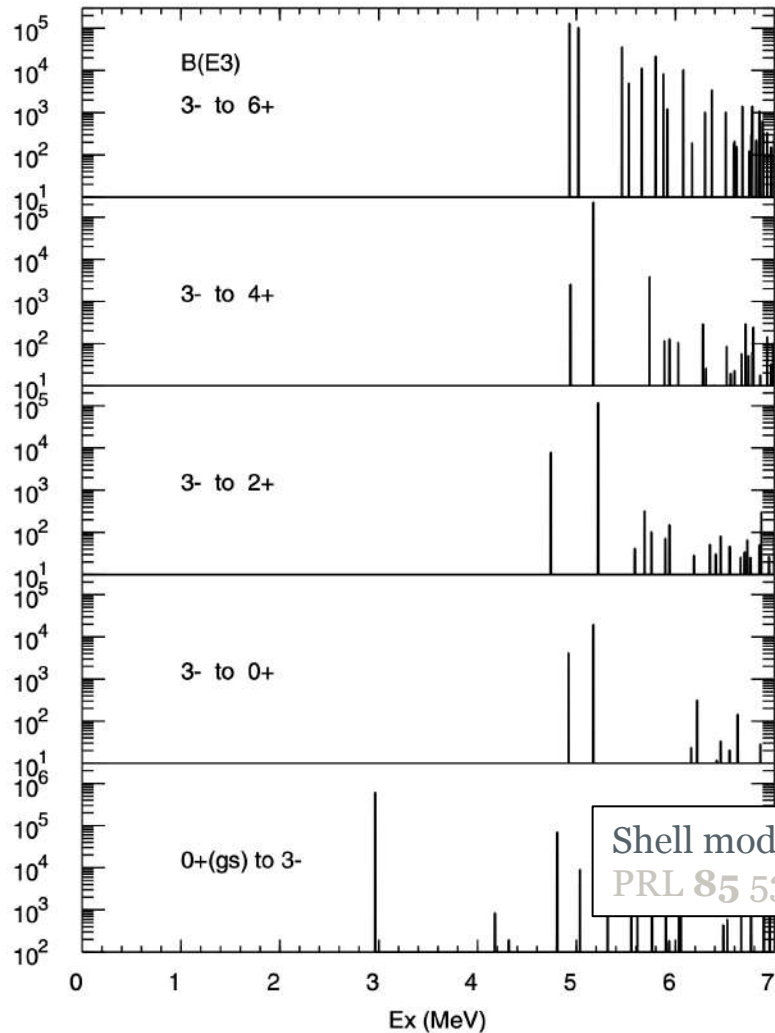
Constrain the data by including literature  $\langle 0_1^+ | E2 | 2_1^+ \rangle$  [ $B(E2; 0_1^+ \rightarrow 2_1^+)$ ] and  $\langle 0_1^+ | E3 | 3_1^- \rangle$  [ $B(E3; 0_1^+ \rightarrow 3_1^-)$ ]

Able to tightly constrain both  $\langle 2_1^+ | E2 | 2_1^+ \rangle$  [ $Q_s(2_1^+)$ ] and  $\langle 3_1^- | E2 | 3_1^- \rangle$  [ $Q_s(3_1^-)$ ]

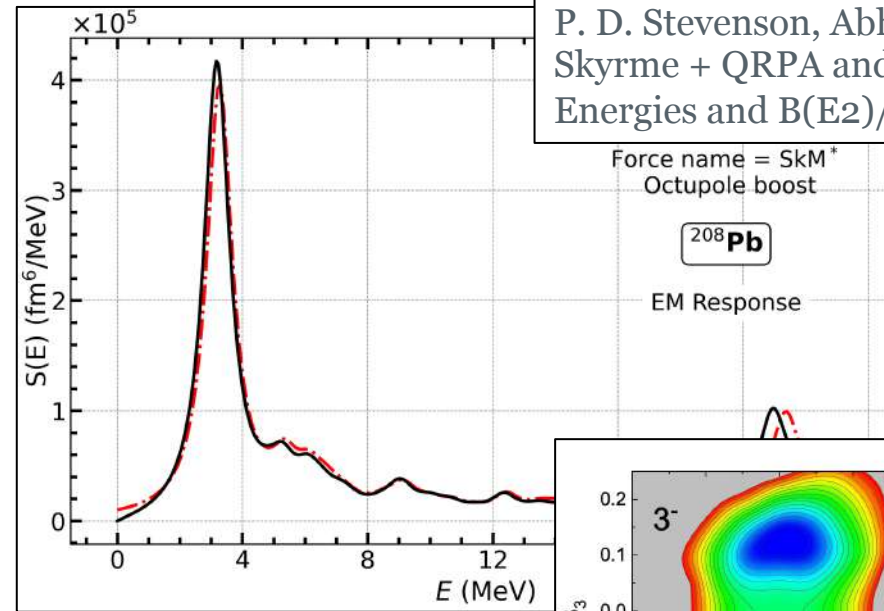
Consistent with Vermeer *et al.* Australian Journal of Physics **37** 123 (1984) but improved uncertainty

JH *et al.* submitted for publication

# Coulomb excitation of $^{208}\text{Pb}$

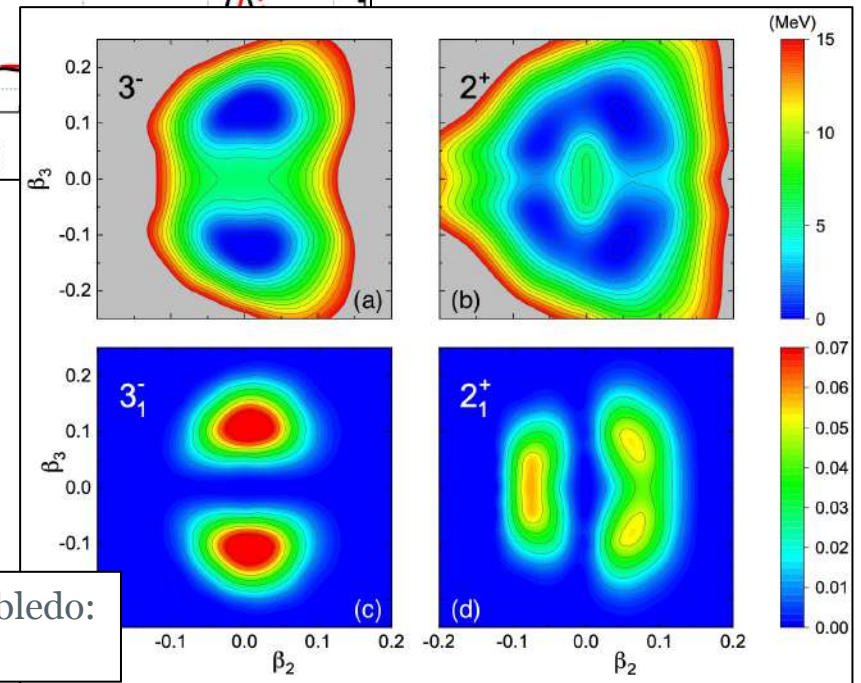


Shell model, B. A. Brown:  
PRL 85 5300 (2020)



P. D. Stevenson, Abhishek, E. Yuksel:  
Skyrme + QRPA and Skyrme + TDHF  
Energies and B(E2)/B(E3) **only**

Model comparison



T. R. Rodriguez and L. Robledo:  
SCCM

JH et al. su

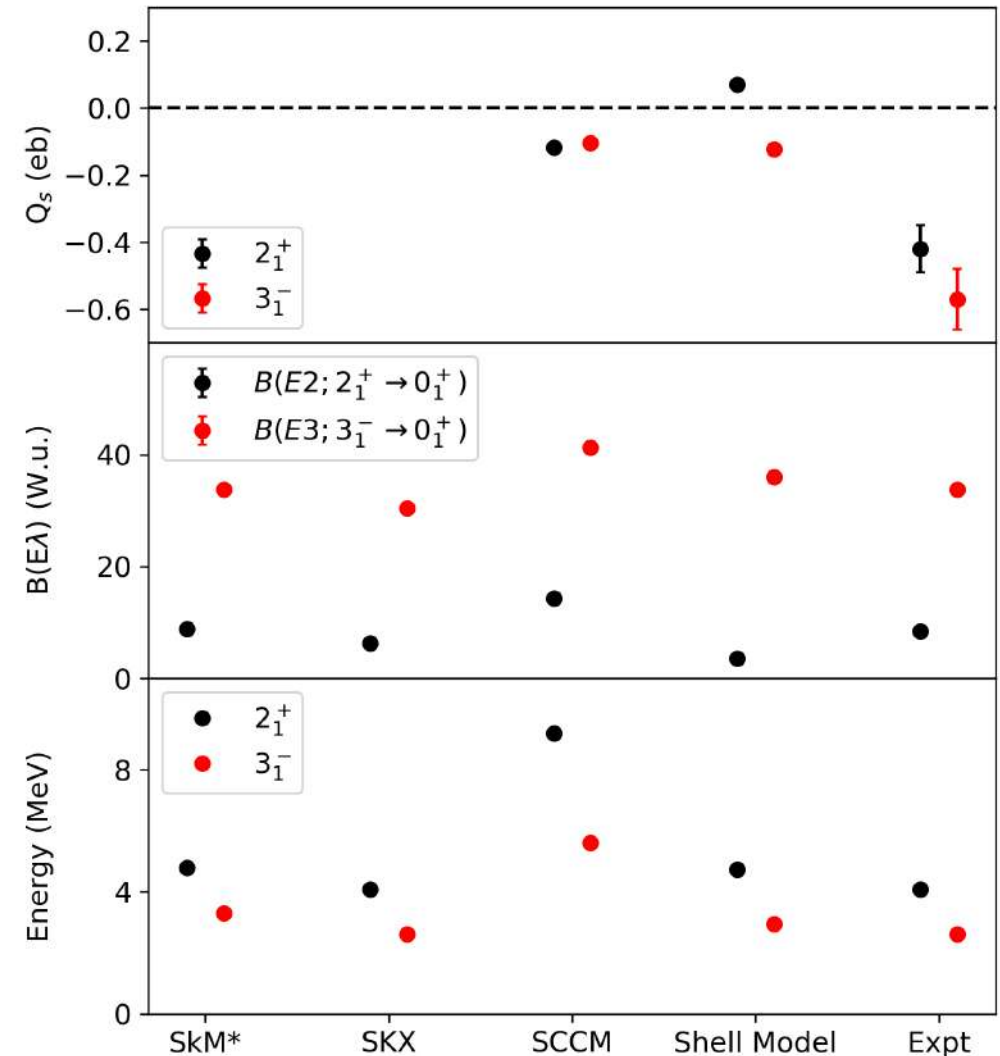
# Coulomb excitation of $^{208}\text{Pb}$

Skyrme models best reproduce  $B(\text{EL})$  and energies but **no**  $Q_s$  values and **no** indication of preference for prolate deformation

SCCM calculations *overpredict* excitation energies and  $B(\text{EL})$  values but **do** reproduce signs and similarity of  $Q_s(2^+)$  and  $Q_s(3^-)$

SM fails to reproduce the signs and magnitudes of the  $Q_s$  values but does reproduce energies and  $B(\text{E}3)$

***No model able to reproduce the electromagnetic observables***



JH *et al.* submitted for publication

# Coulomb excitation of $^{208}\text{Pb}$

Skyrme models best reproduce B(EL) and energies but **no**  $Q_s$  values and **no** indication of preference for prolate deformation

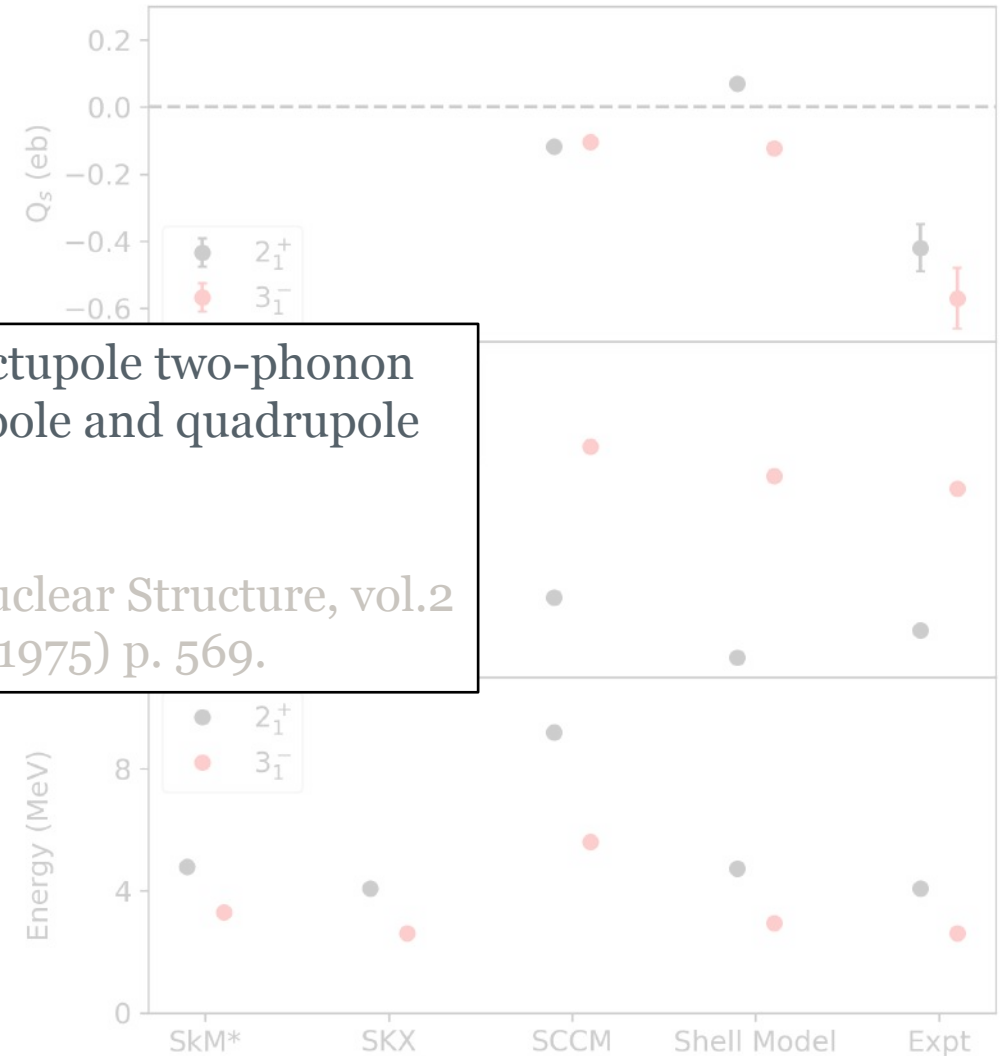
SCCM calculations overpredict  $Q_s(2^+)$  and B(EL) values but do not show the similarity of  $Q_s(2^+)$  and  $Q_s(3^-)$

SM fails to reproduce the  $Q_s$  values but does reproduce energies and B(E3)

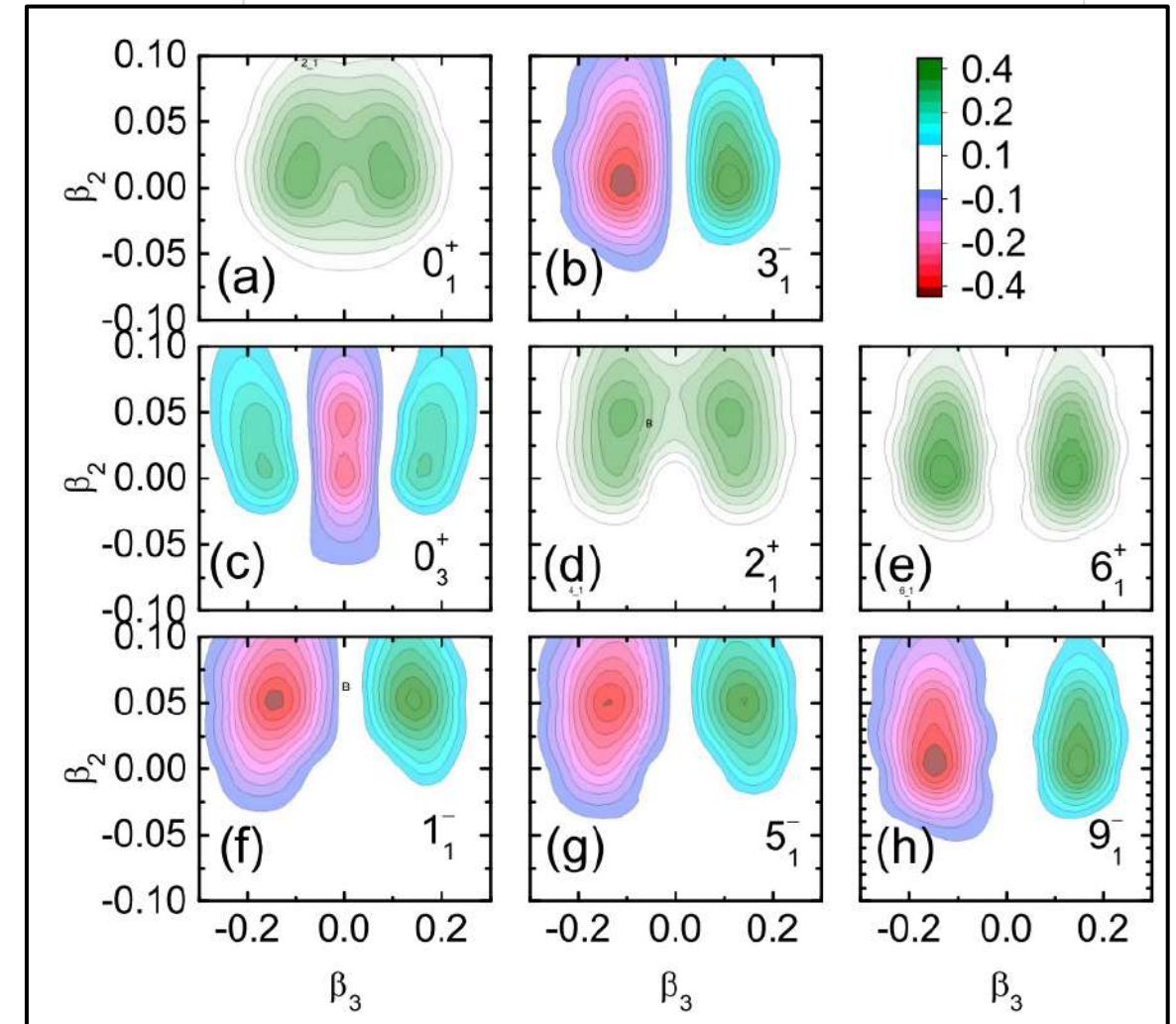
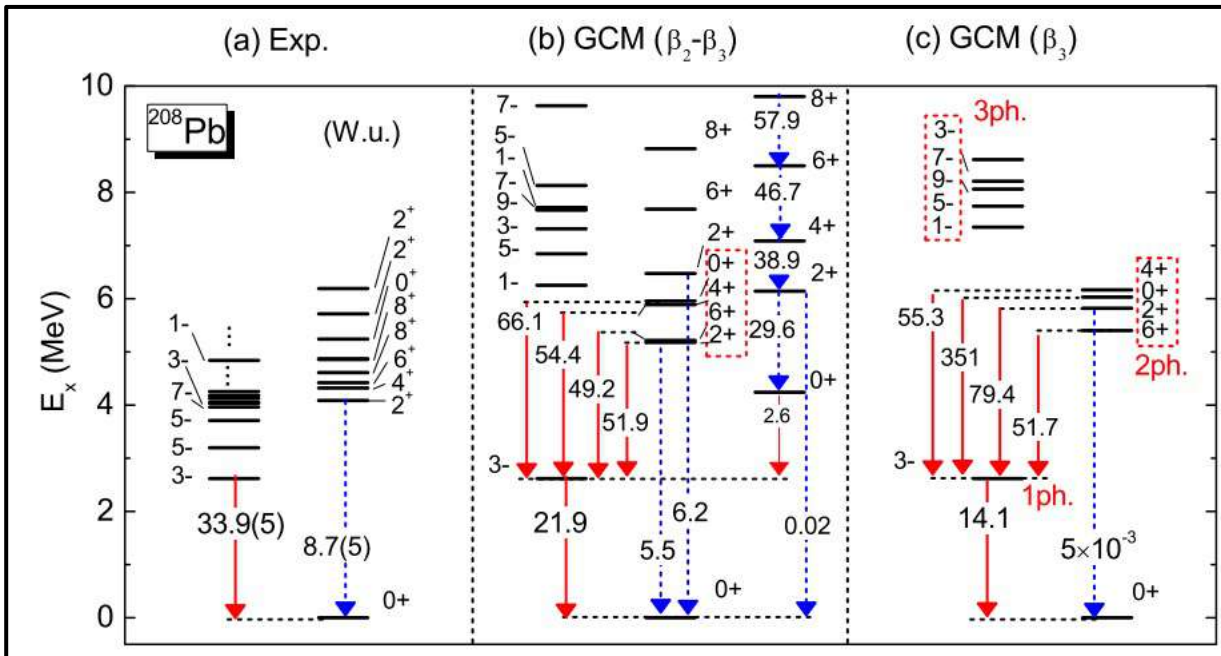
*No model able to reproduce the electromagnetic observables*

Implications for splitting of octupole two-phonon states due to coupling of octupole and quadrupole modes

A. Bohr and B. R. Mottelson, Nuclear Structure, vol.2 (Benjamin, New York, 1975) p. 569.



# Coulomb excitation of $^{208}\text{Pb}$



the  $Q_s$  values but does reproduce energies and  $B(E3)$

Yao and Hagino [PRC **94** 011303(R) (2016)]

Investigated quadrupole-octupole mixing in GCM

With thanks to:

J. Henderson,<sup>1,\*</sup> J. Heery,<sup>1</sup> M. Rocchini,<sup>2,3</sup> M. Siciliano,<sup>4</sup> N. Sensharma,<sup>4</sup> A. D. Ayangeakaa,<sup>5,6</sup>  
R. V. F. Janssens,<sup>5,6</sup> T. M. Kowalewski,<sup>5,6</sup> Abhishek,<sup>1</sup> P. D. Stevenson,<sup>1</sup> E. Yuksel,<sup>1</sup> B. A. Brown,<sup>7,8</sup>  
T. R. Rodriguez,<sup>9,10,11</sup> L. M. Robledo,<sup>10,11,12</sup> C. Y. Wu,<sup>13</sup> S. Kisyov,<sup>13,†</sup> C. Müller-Gatermann,<sup>4</sup>  
V. Bildstein,<sup>3</sup> L. Canete,<sup>1</sup> C. M. Campbell,<sup>14</sup> S. Carmichael,<sup>15</sup> M. P. Carpenter,<sup>4</sup> W. N. Catford,<sup>1</sup>  
P. Copp,<sup>4,‡</sup> C. Cousins,<sup>1</sup> M. Devlin,<sup>16</sup> D. T. Doherty,<sup>1</sup> P. E. Garrett,<sup>3</sup> U. Garg,<sup>15</sup> L. P. Gaffney,<sup>17</sup>  
K. Hadynska-Klek,<sup>18</sup> D. J. Hartley,<sup>19</sup> S. F. Hicks,<sup>20,21</sup> H. Jayatissa,<sup>4,‡</sup> S. R. Johnson,<sup>5,6</sup> D. Kalaydjieva,<sup>22</sup>  
F. Kondev,<sup>4</sup> D. Lascar,<sup>23</sup> T. Lauritsen,<sup>4</sup> G. Lotay,<sup>1</sup> N. Marchini,<sup>2</sup> M. Matejska-Minda,<sup>24</sup> S. Nandi,<sup>4</sup>  
A. Nannini,<sup>2</sup> C. O'Shea,<sup>1</sup> S. Pascu,<sup>1,25</sup> C. Paxman,<sup>1</sup> A. Perkoff,<sup>26</sup> E. E. Peters,<sup>20</sup> Zs. Podolyák,<sup>1</sup> A. Radich,<sup>3</sup>  
R. Rathod,<sup>15</sup> B. J. Reed,<sup>1,§</sup> P. H. Regan,<sup>1,27</sup> W. Reviol,<sup>4</sup> E. Rubino,<sup>7,¶</sup> R. Russell,<sup>1</sup> D. Seweryniak,<sup>4</sup>  
J. R. Vanhoy,<sup>19</sup> G. L. Wilson,<sup>4,28,\*\*</sup> K. Wrzosek-Lipska,<sup>18</sup> S. Yates,<sup>5,6</sup> S. W. Yates,<sup>20</sup> and I. Zanon<sup>29</sup>

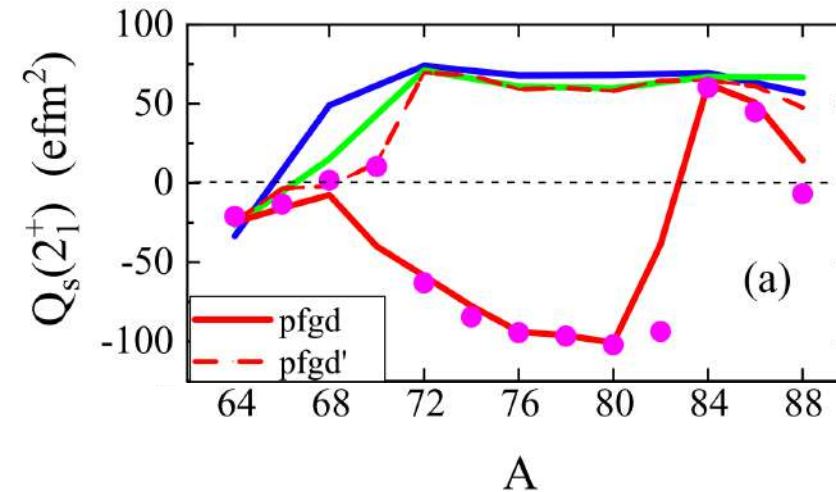
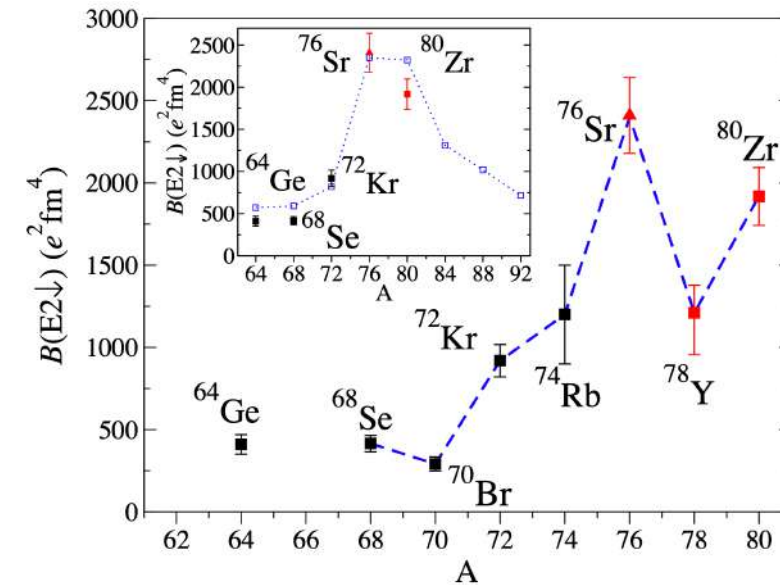
# Strontium-80 Coulomb excitation

Region around  $N=Z=40$  ( $^{80}\text{Zr}$ ) associated with strong deformation

Driven by quasi-SU3 symmetry - strong  $\langle Q \cdot Q \rangle$  interaction between  $g_{9/2}$  and  $d_{5/2}$  orbitals

Completely erases the influence of the HO shell closure (i.e.  $^{90}\text{Zr}$ )

Predictions from PMMU interaction of a region of *prolate* deformation



R. Llewellyn *et al.*  
 PRL 124 152501 (2020)

K. Kaneko *et al.*  
 PLB 817 136286 (2021)

# Strontium-80 Coulomb excitation

Region around  $N=Z=40$  ( $^{80}\text{Zr}$ ) associated with strong deformation

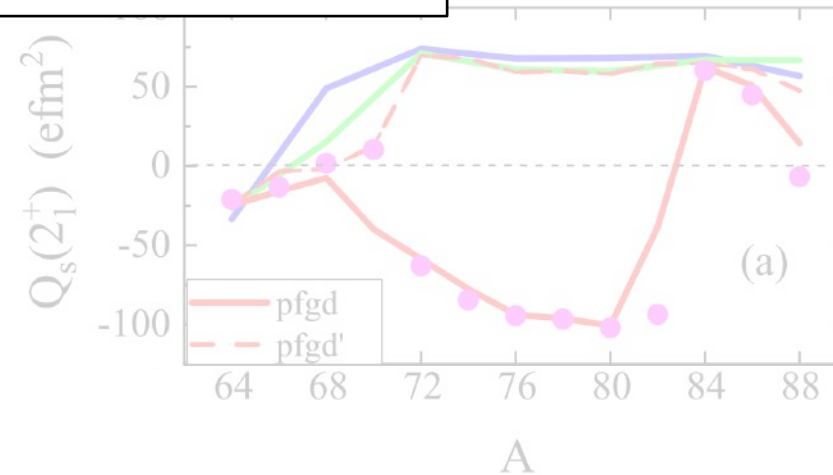
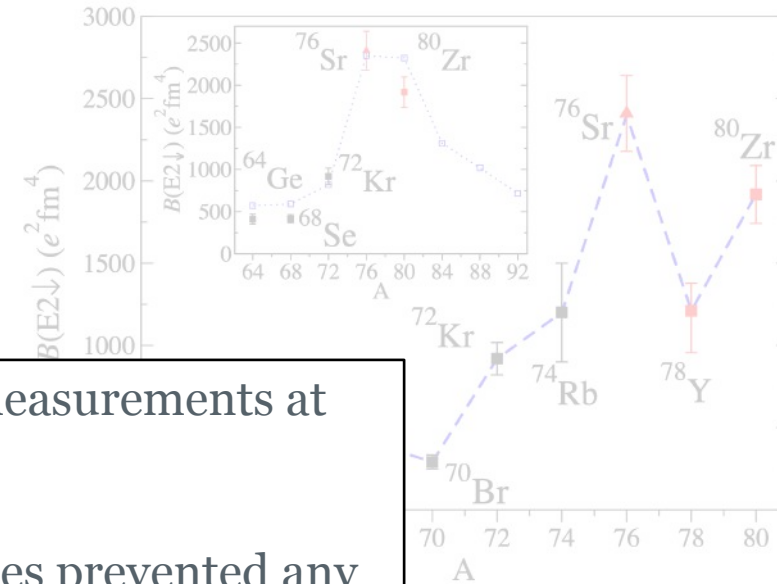
Driven by quasi-SU3 symmetry, strong  $(\rho, \rho)$  interaction between  $g_{9/2}$  &  $g_{7/2}$

Completely erases the influence of shell closure (i.e.  $^{90}\text{Zr}$ )

Predictions from PMMU interaction of a region of *prolate* deformation

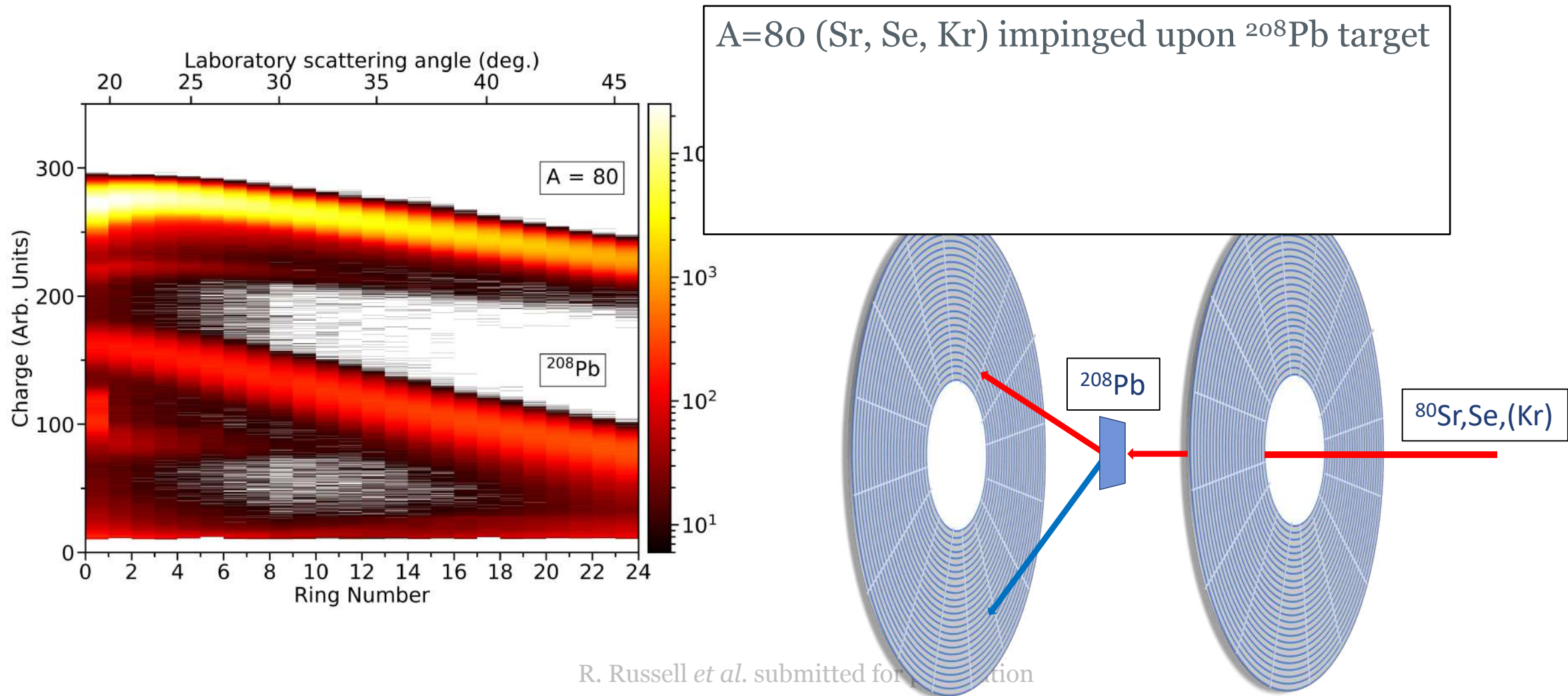
**Motivated Coulomb excitation measurements at TRIUMF**

Goals were  $^{78,80}\text{Sr}$  - beam difficulties prevented any attempt at  $^{78}\text{Sr}$  (JANUS @ ReA6, FRIB PAC34 🙅)

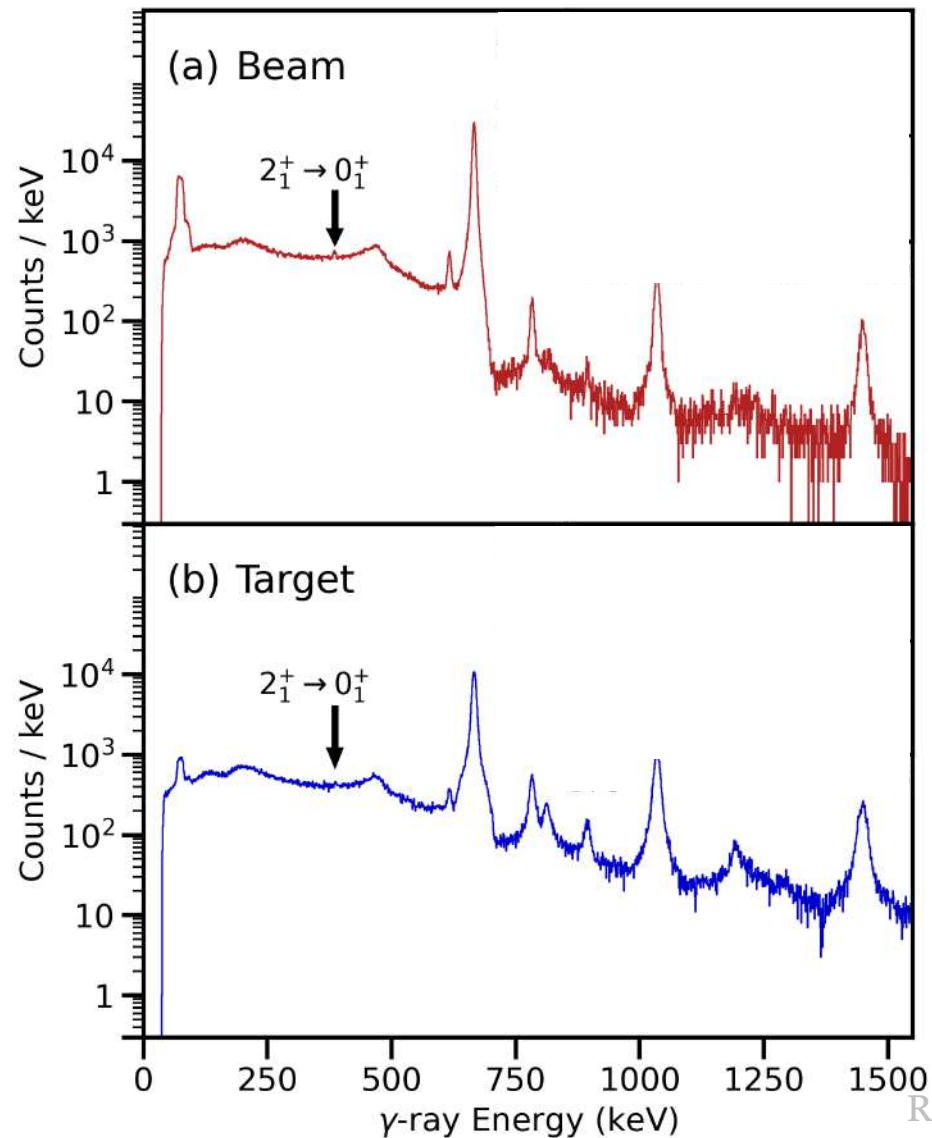


R. Llewellyn *et al.*  
PRL 124 152501 (2020)

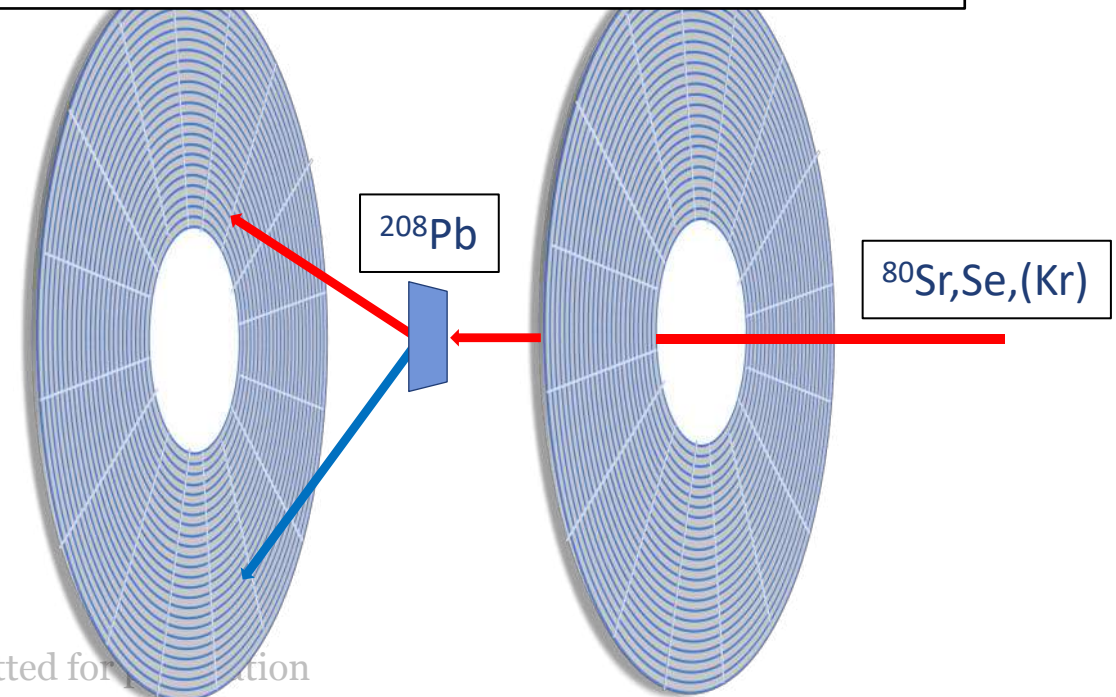
K. Kaneko *et al.*  
PLB 817 136286 (2021)



# Strontium-80 Coulomb excitation

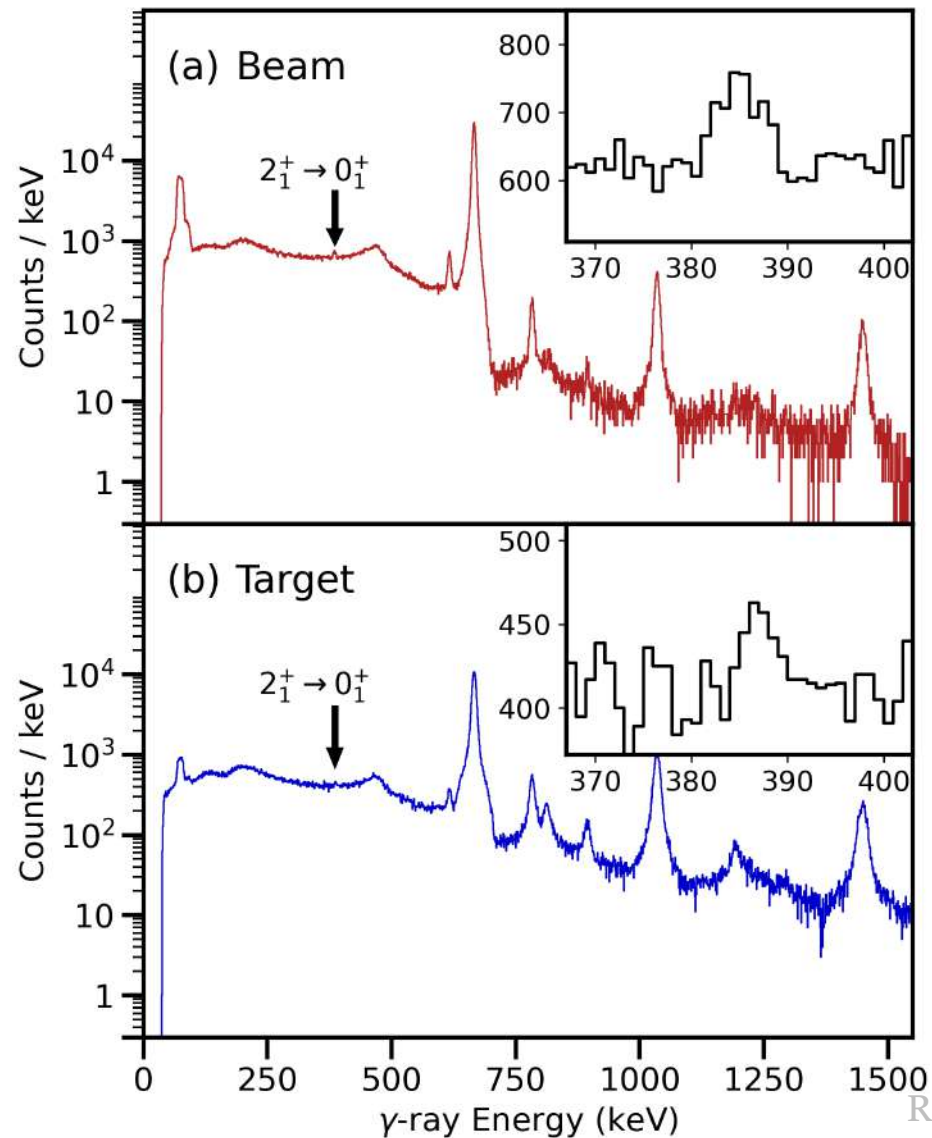


A=80 (Sr, Se, Kr) impinged upon  $^{208}\text{Pb}$  target  
 Spectra dominated by  $^{80}\text{Se}$  Coulomb excitation



R. Russell *et al.* submitted for publication

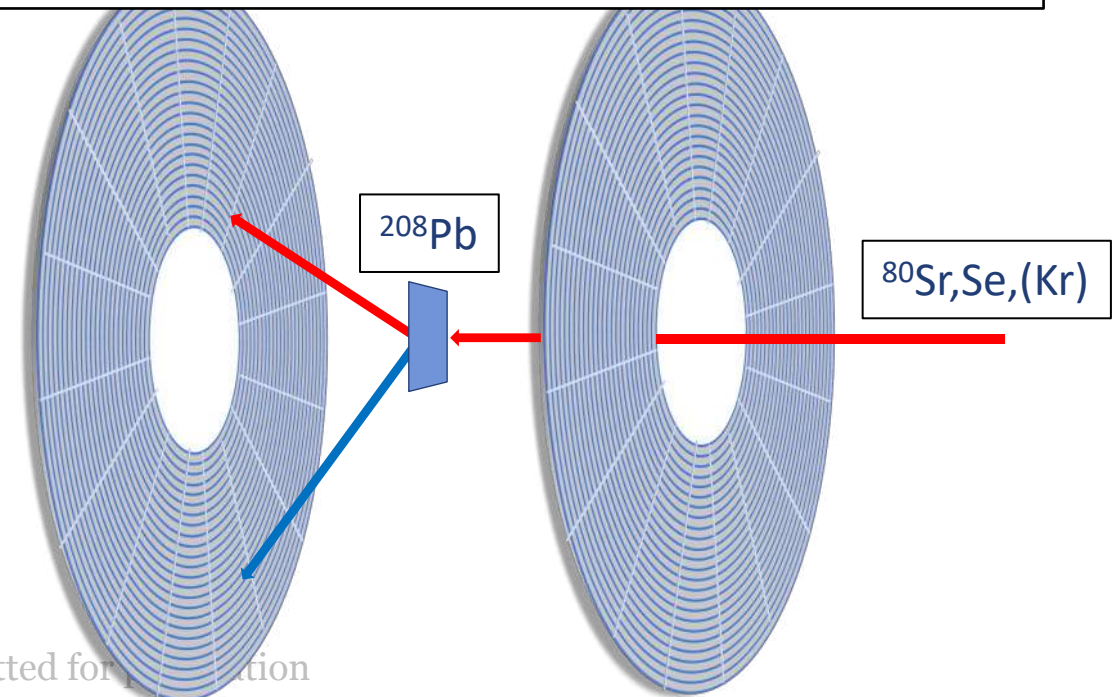
# Strontium-80 Coulomb excitation



A=80 (Sr, Se, Kr) impinged upon  $^{208}\text{Pb}$  target

Spectra dominated by  $^{80}\text{Se}$  Coulomb excitation

$^{80}\text{Sr}$   $2_1^+ \rightarrow 0_1^+$  visible on  $^{80}\text{Se}$  Compton background



R. Russell *et al.* submitted for publication

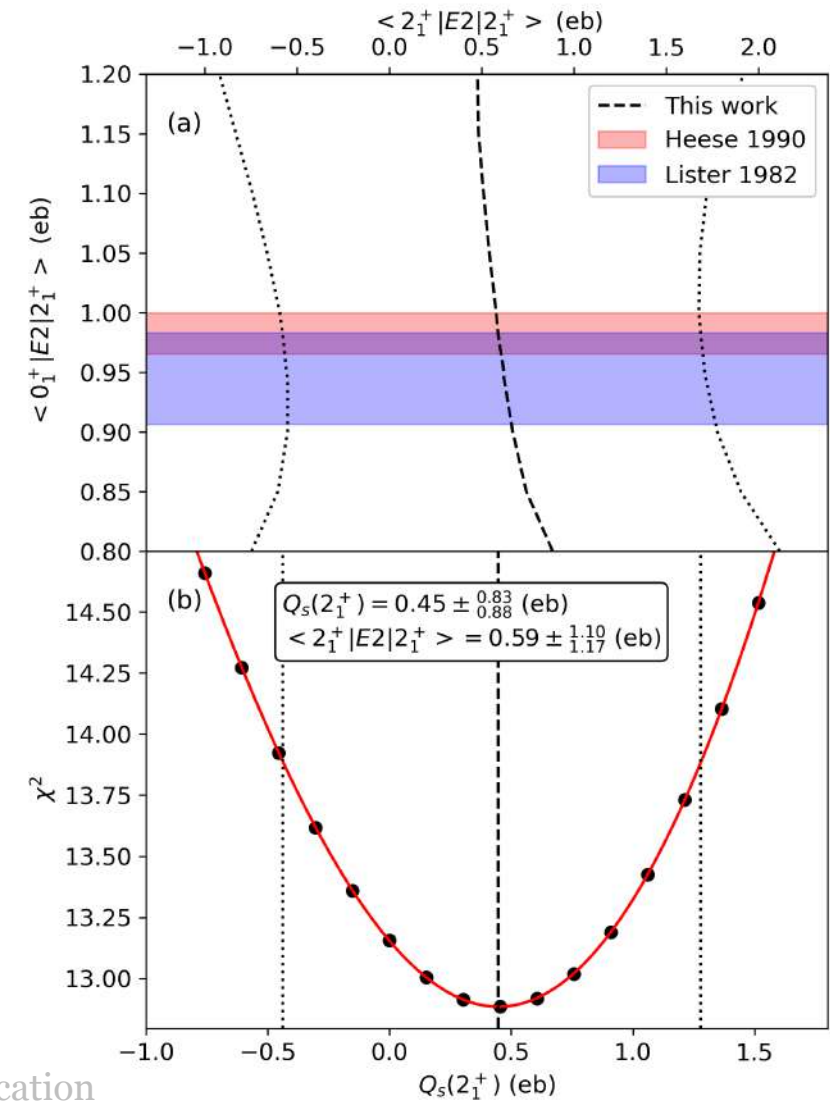
# Strontium-80 Coulomb excitation

Strontium-80 quadrupole moment extracted from angular distribution

Verified consistency with both literature  $2_1^+$  state lifetimes

Limited correlation between  $\langle 0_1^+ | E2 | 2_1^+ \rangle$  and  $\langle 2_1^+ | E2 | 2_1^+ \rangle$

Large uncertainty dominated by background from  $^{80}\text{Se}$  Coulomb excitation

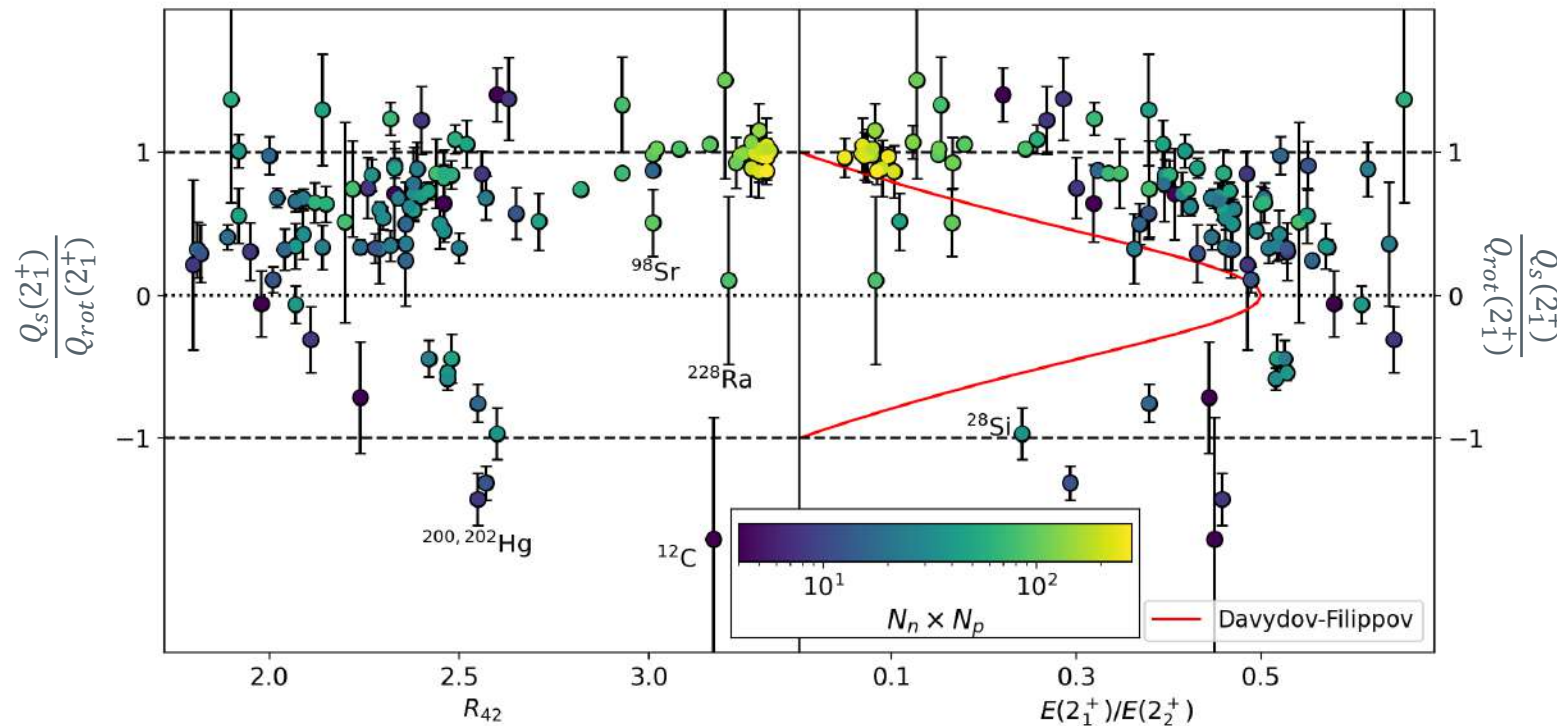


R. Russell *et al.* submitted for publication

# Strontium-80 Coulomb excitation

Use a simple metric for the form of the nuclear deformation

$$Q_{rot}(2_1^+) = \frac{2}{7} \sqrt{\frac{16\pi}{5} B(E2; 0_1^+ \rightarrow 2_1^+)}$$



$$\cos(3\gamma) \approx -\frac{Q_s(2_1^+)}{Q_{rot}(2_1^+)} = q_s$$

JH, PRC **102** 054306 (2020)

Rhodes *et al.* PRC **103** L051301 (2021)

# Strontium-80 Coulomb excitation

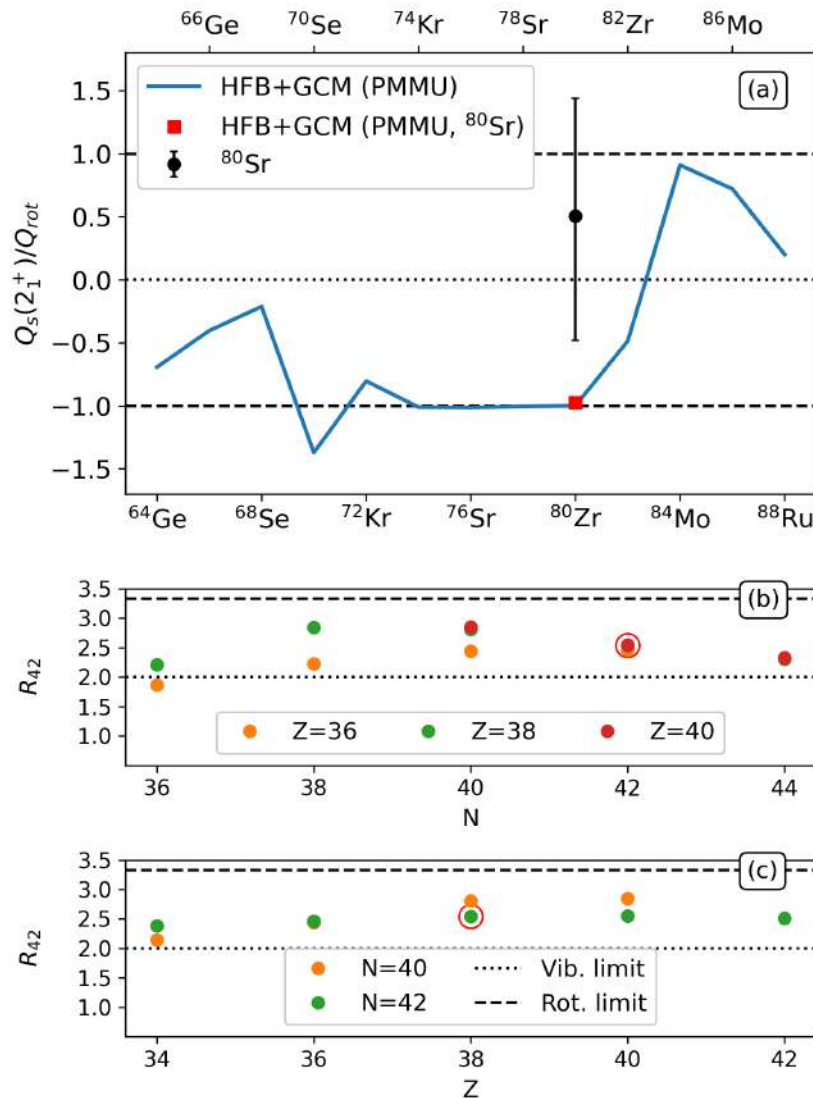
Comparison with PMMU calculations

Predict near-axial, prolate systems around  $N=Z=40$

$$\frac{Q_s(2_1^+)}{Q_{s,rot}(2_1^+)} \approx -1$$

Even with large uncertainty, experimental  $Q_s(2_1^+)$  is **inconsistent** with this prediction

More consistent with *triaxial* or *oblate* deformations



R. Russell *et al.* submitted for publication

## Strontium-80 Coulomb excitation

Contrary to PMMU calculation predictions,  $^{80}\text{Sr}$  appears to be *triaxial* or *oblate*

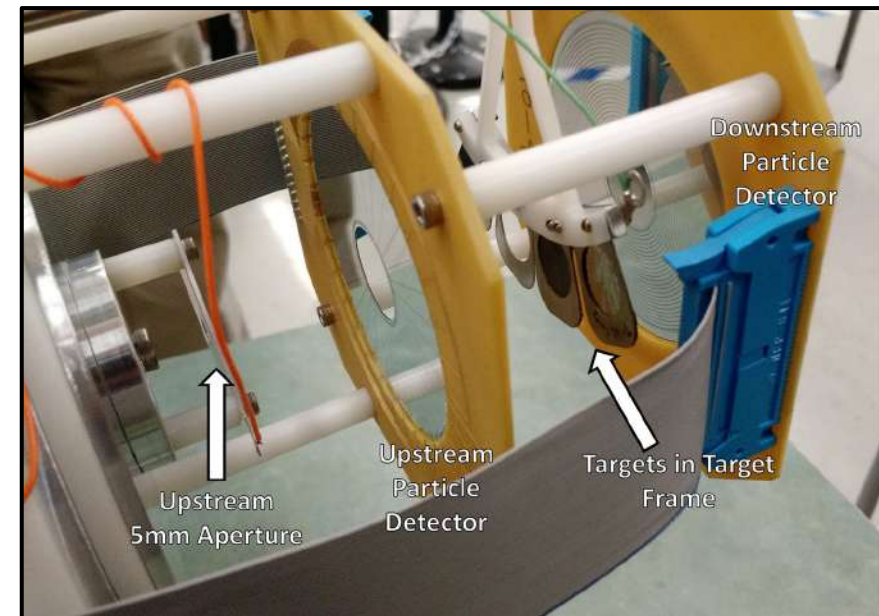
Any island of strong, prolate, axial deformation around  $N=Z=40$  is confined to  $^{76,78}\text{Sr}$  and  $^{78,80}\text{Zr}$

Recently presented (as-yet unpublished) SM results imply a different mechanism – more varied shapes

### JANUS – A setup for low-energy Coulomb excitation at ReA3 ☆

E. Lunderberg<sup>a,b</sup>, J. Belarge<sup>a,1</sup>, P.C. Bender<sup>a</sup>, B. Bucher<sup>c</sup>, D. Cline<sup>d</sup>, B. Elman<sup>a,b</sup>, A. Gade<sup>a,b</sup> ✉  
, S.N. Liddick<sup>a,e</sup>, B. Longfellow<sup>a,b</sup>, C. Prokop<sup>a,e</sup>, D. Weisshaar<sup>a</sup>, C.Y. Wu<sup>c</sup>

Neutron-deficient Sr (should be) accessible at FRIB-ReA6: a priority to perform safe Coulomb excitation



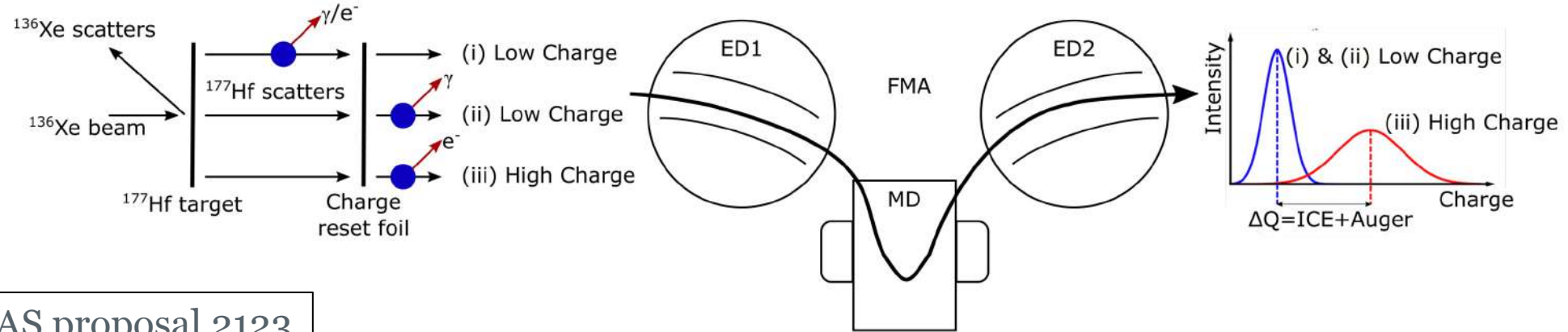
With thanks to:

R. Russell<sup>a</sup>, J. Heery<sup>a</sup>, J. Henderson<sup>a,\*</sup>, R. Wadsworth<sup>b</sup>, K. Kaneko<sup>c</sup>, N. Shimizu<sup>d</sup>, T. Mizusaki<sup>e</sup>, Y. Sun<sup>f</sup>, C. Andreoiu<sup>h</sup>,  
D. W. Annen<sup>h</sup>, A. A. Avaa<sup>i</sup>, G. C. Ball<sup>i</sup>, V. Bildstein<sup>j</sup>, S. Buck<sup>j</sup>, C. Cousins<sup>a</sup>, A. B. Garnsworthy<sup>i</sup>, S. A. Gillespie<sup>k</sup>, B. Greaves<sup>j</sup>,  
A. Grimes<sup>i</sup>, G. Hackman<sup>i</sup>, R. O. Hughes<sup>l</sup>, D. G. Jenkins<sup>b</sup>, T. M. Kowalewski<sup>m,n</sup>, M. S. Martin<sup>g</sup>, C. Müller-Gatermann<sup>o</sup>,  
J. R. Murias<sup>i</sup>, S. Murillo-Morales<sup>i</sup>, S. Pascu<sup>a,p</sup>, D. M. Rhodes<sup>i,l</sup>, J. Smallcombe<sup>q</sup>, P. Spagnoletti<sup>h</sup>, C. E. Svensson<sup>i,j</sup>, B. Wallis<sup>b</sup>,  
J. Williams<sup>i</sup>, C. Y. Wu<sup>l</sup>, D. Yates<sup>i,r</sup>

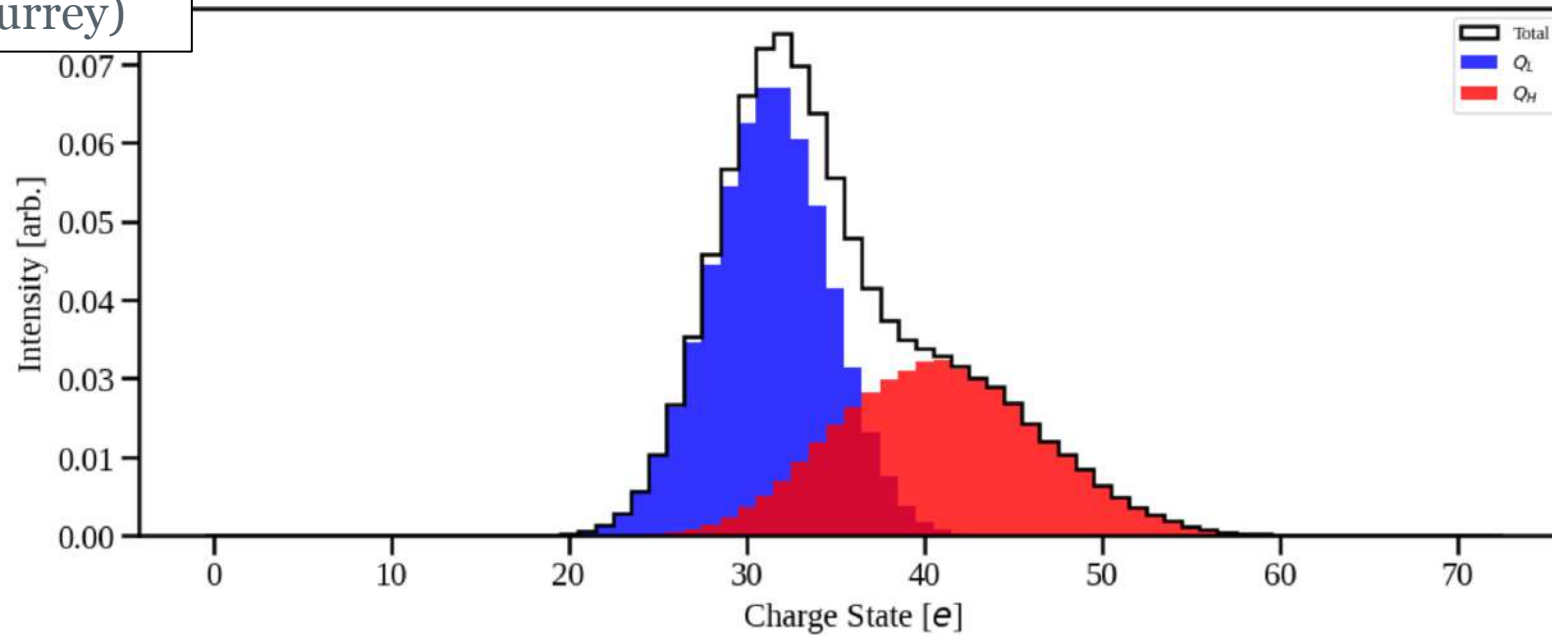


# Coulomb excitation as a tool for nuclear medicine

# Coulomb excitation as a tool for nuclear medicine



ANL ATLAS proposal 2123  
PI: Jacob Heery (Surrey)



## Charge-state distribution measurements

Scattered beam from  $^{136}\text{Xe}$  caused issues at FMA focal plane – challenging to interpret online data

Changed the beam/target combination to  $^{40}\text{Ar}/^{197}\text{Au}$

Almost a repeat of the FMA/EMMA commissioning experiments

Lighter beam + heavier target massively reduced scattered beam at FMA focal plane

S3-detector at backwards angles to provide normalisation (potential for CoulEx measurement of  $^{40}\text{Ar}$ ?)

# Charge-state distribution measurements

## Method:

Reset foil (carbon) located at  $\sim 1$  cm from target

Recoiling Au ions at  $\sim 80$  MeV ( $\sim 0.9$  cm/ns)

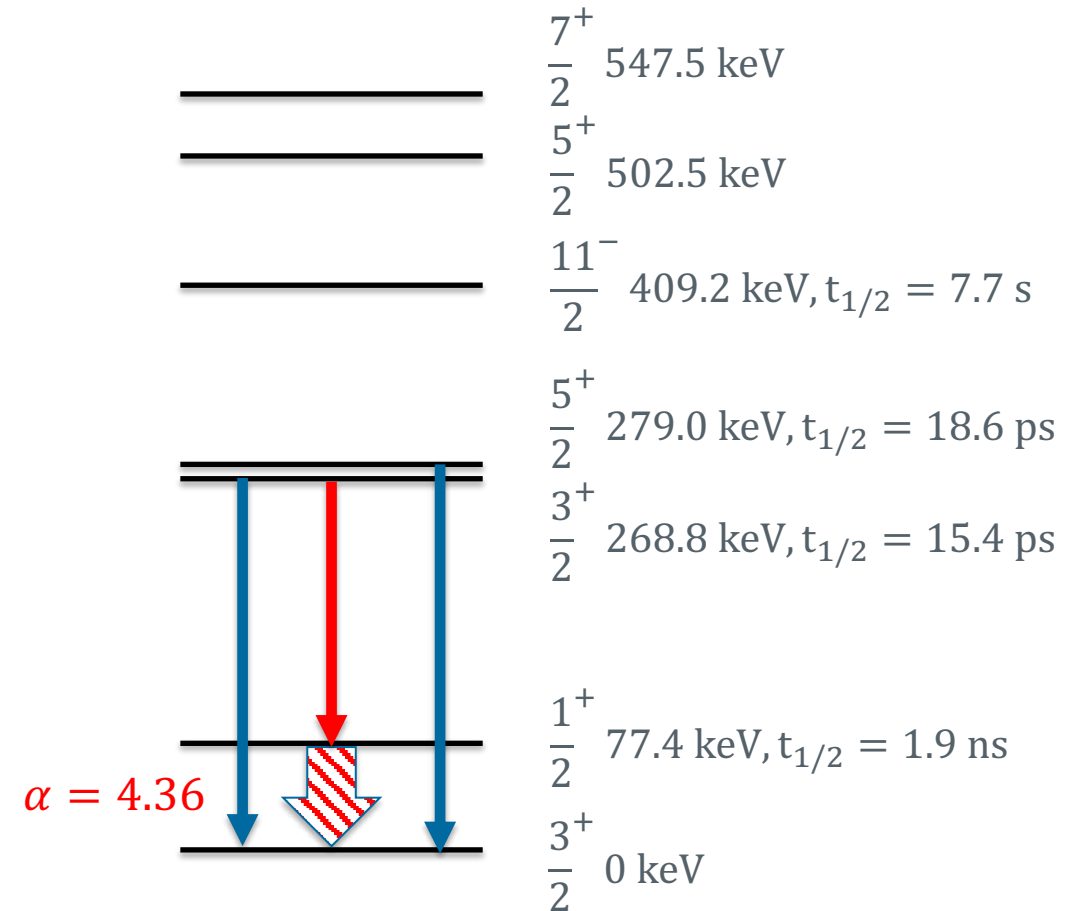
All states above 77 keV have half-lives  $\sim 10$  ps or lower

Gate on 191-keV gamma-ray populating 77-keV state

Measure charge state

Will have low-charge (gamma-decay and IC before reset) and high-charge (IC after foil) component

Centroid difference between HC and LC gives mean Auger-electron multiplicity



# Charge-state distribution measurements

Method:

Reset foil

Recoiling

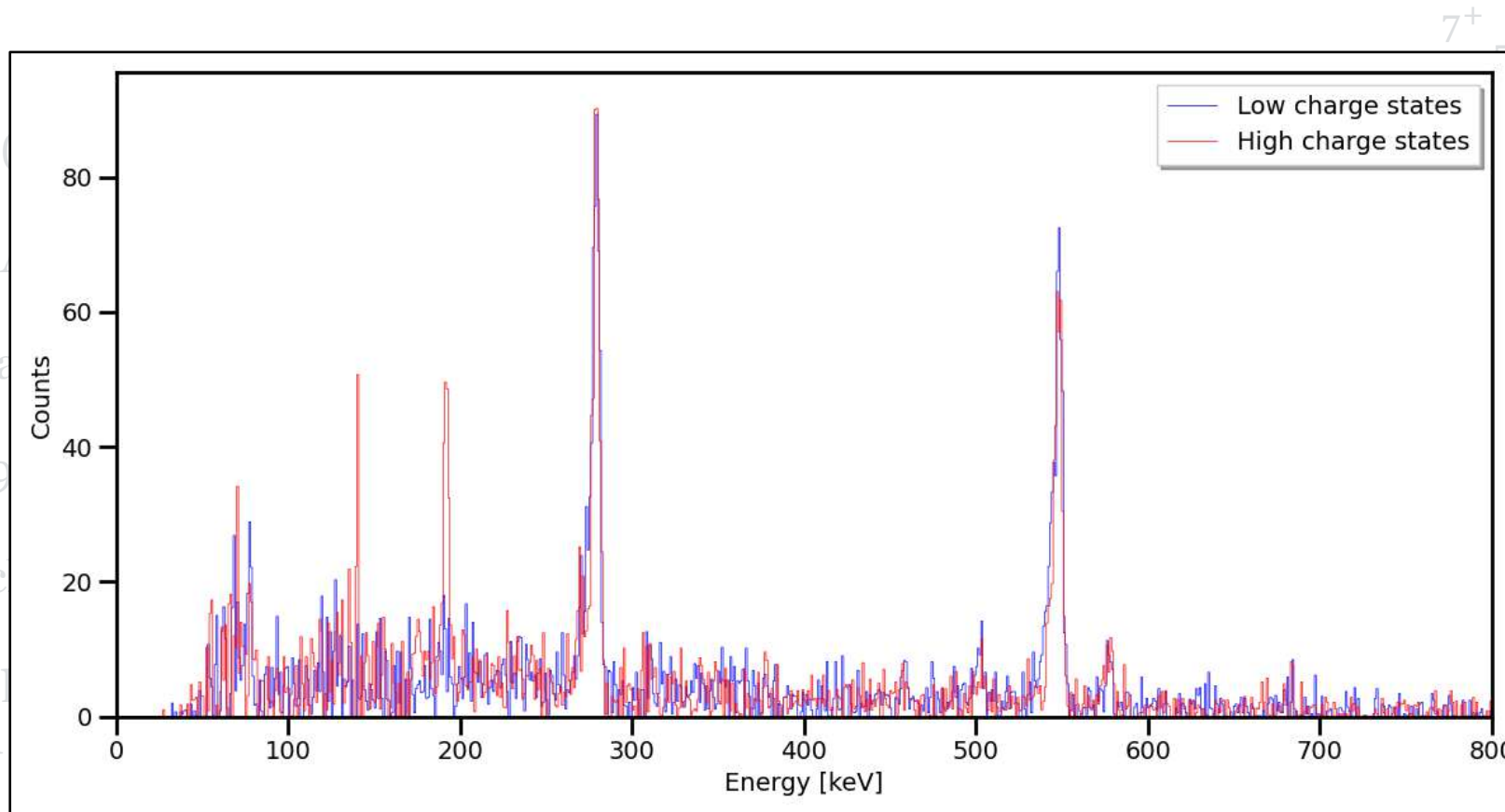
All states

Gate on

Measure

Will have  
 (reset) and

Centroid difference between HC and LC gives mean  
 Auger-electron multiplicity



$7^+$   
 17.5 keV

2.5 keV

9.2 keV,  $t_{1/2} = 7.7$  s

9.0 keV,  $t_{1/2} = 18.6$  ps

8.8 keV,  $t_{1/2} = 15.4$  ps

4 keV,  $t_{1/2} = 1.9$  ns

2.5 keV

# Charge-state distribution measurements

## Method:

Reset foil (carbon)

Recoiling Au ion

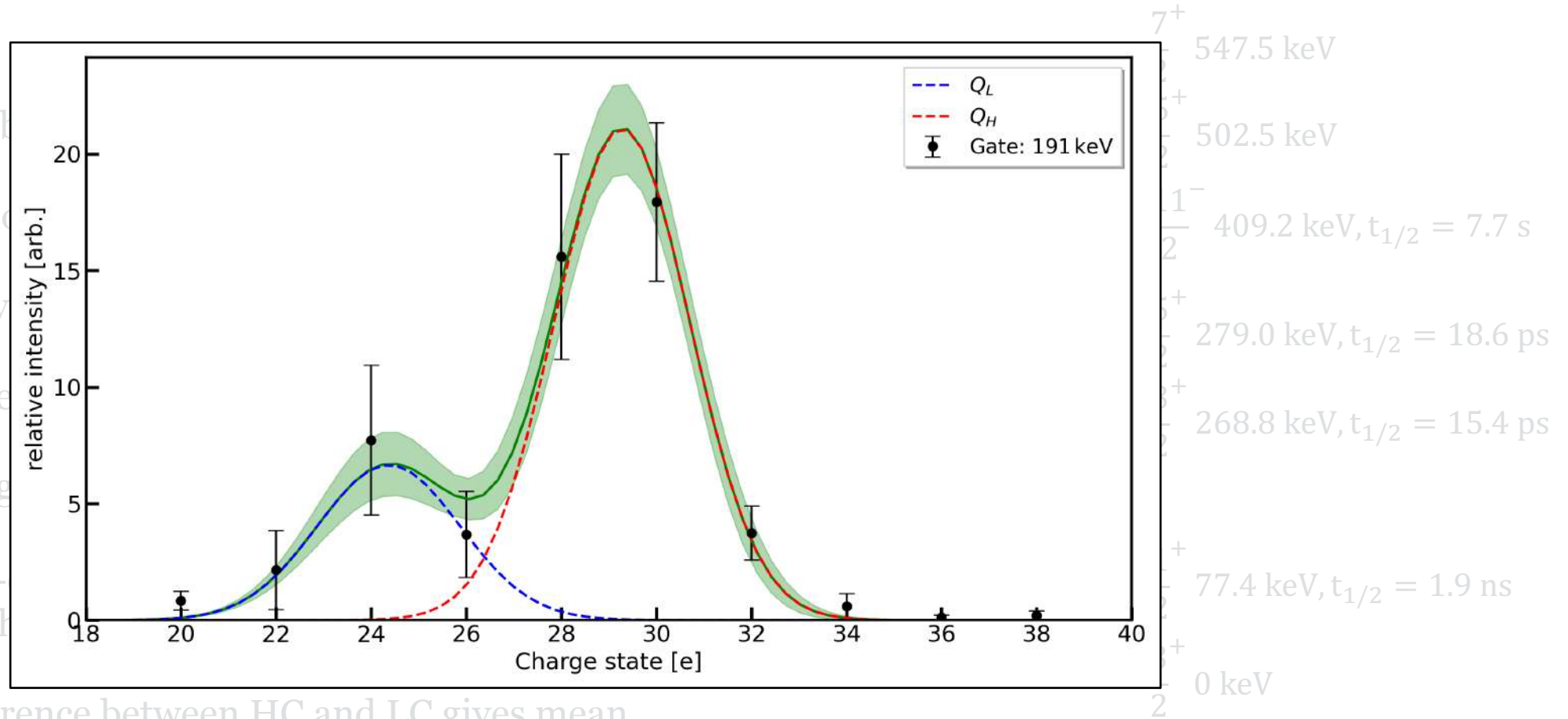
All states above

Gate on 191-keV

Measure charge

Will have low-  
reset) and high

Centroid difference between HC and LC gives mean  
Auger-electron multiplicity



# Charge-state distribution measurements

## Method:

Reset foil (carbon)

Recoiling Au ion

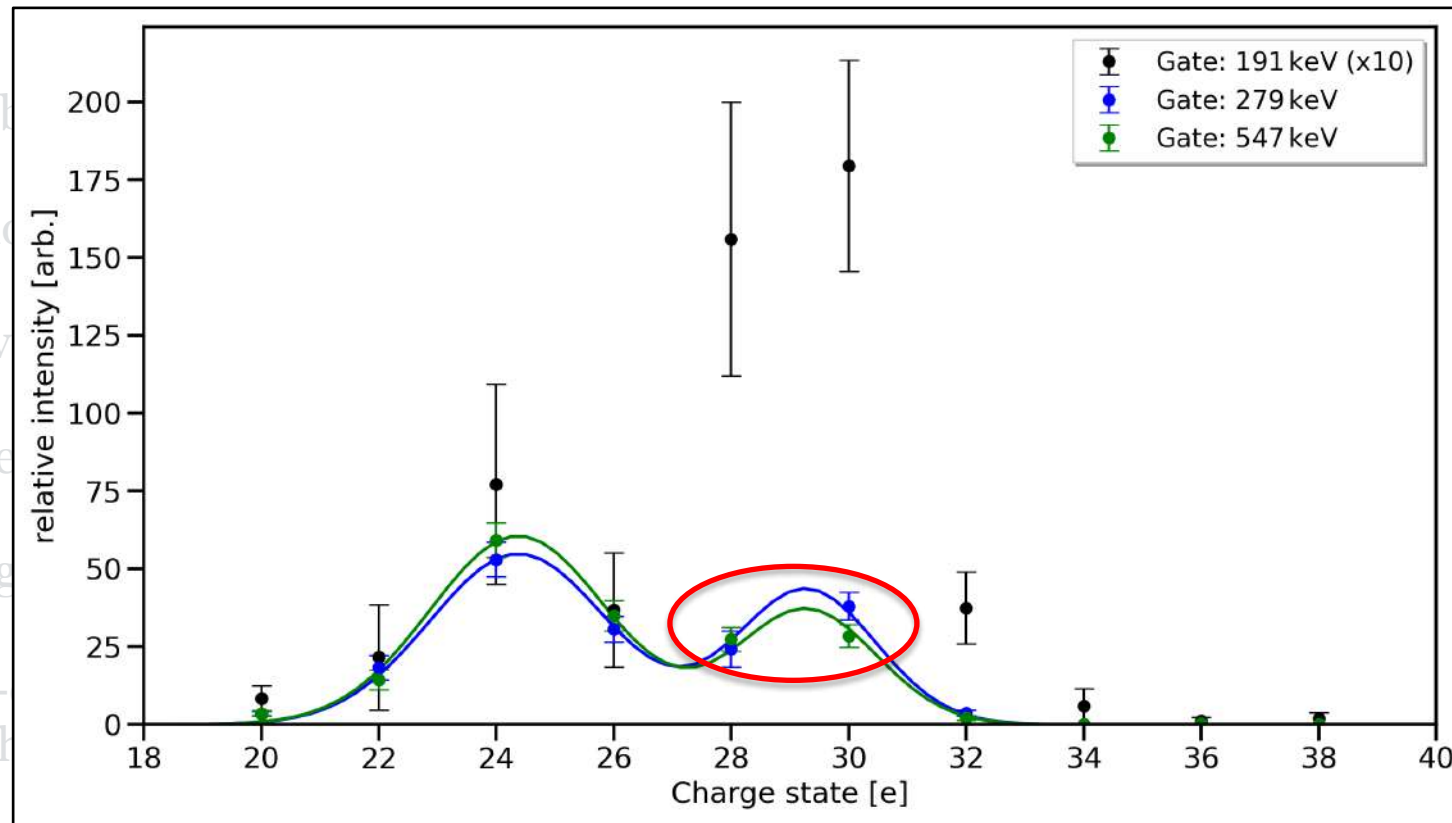
All states above

Gate on 191-keV

Measure charge

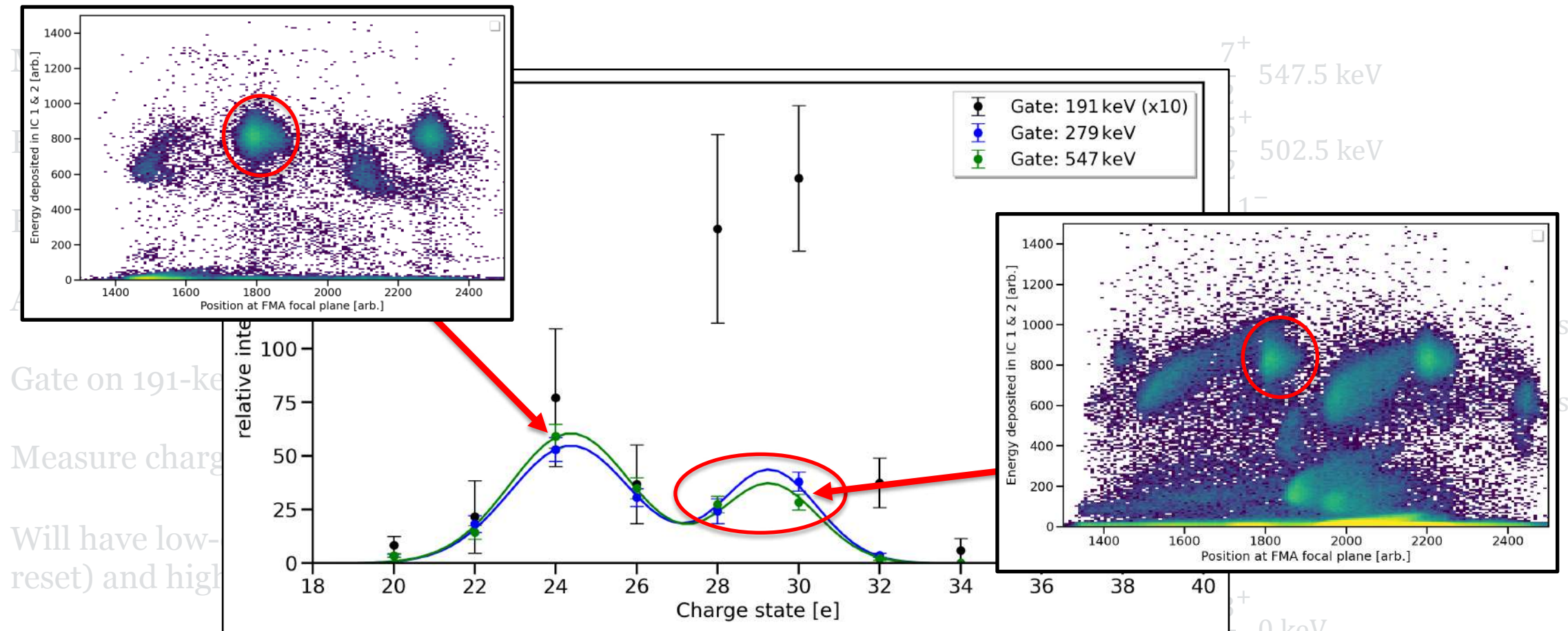
Will have low-  
reset) and high

Centroid difference between HC and LC gives mean  
Auger-electron multiplicity



7<sup>+</sup> 547.5 keV  
 6<sup>+</sup> 502.5 keV  
 5<sup>+</sup> 409.2 keV,  $t_{1/2} = 7.7$  s  
 4<sup>+</sup> 279.0 keV,  $t_{1/2} = 18.6$  ps  
 3<sup>+</sup> 268.8 keV,  $t_{1/2} = 15.4$  ps  
 2<sup>+</sup> 77.4 keV,  $t_{1/2} = 1.9$  ns  
 1<sup>+</sup> 0 keV  
 2<sup>-</sup>

# Charge-state distribution measurements



Gate on 191-keV

Measure charge

Will have low-  
 reset) and high

Centroid difference between HC and LC gives mean  
 Auger-electron multiplicity

With thanks to:

J. Heery<sup>1,2</sup>, J. Henderson<sup>1</sup>, T. Budner<sup>3</sup>, M.P. Carpenter<sup>3</sup>, W. Catford<sup>1</sup>, J. Chadderton<sup>4</sup>,  
R. Chakma<sup>3</sup>, S. Collins<sup>2</sup>, C. Cousins<sup>1</sup>, J. Cubiss<sup>5</sup>, A. Dewald<sup>6</sup>, D. Doherty<sup>1</sup>, F. Dunkel<sup>6</sup>, S. Dutta<sup>7</sup>,  
A. Ertoprak<sup>3</sup>, C. Fransen<sup>6</sup>, R.-D. Herzberg<sup>4</sup>, V. Karayoncev<sup>3</sup>, B. Kay<sup>3</sup>, T. Kibédi<sup>8</sup>, F. G. Kondev<sup>3</sup>,  
C.-D. Lakenbrink<sup>6</sup>, T. Lauritsen<sup>3</sup>, G. Lorusso<sup>2</sup>, G. Lotay<sup>1</sup>, C. Müller-Gatermann<sup>3</sup>, B. S. Nara  
Singh<sup>7</sup>, J. Nolan<sup>3</sup>, D O'Donnell<sup>7</sup>, E. O'Sullivan<sup>1,2</sup>, S. Pascu<sup>1</sup>, Z. Podolyák<sup>1</sup>, P. H. Regan<sup>1,2</sup>,  
A. Renne<sup>3</sup>, W. Reviol<sup>3</sup>, R. Russell<sup>1</sup>, J. Sarén<sup>9</sup>, N. Sensharma<sup>3</sup>, D. Seweryniak<sup>3</sup>, R. Shearman<sup>2</sup>,  
M. Siciliano<sup>3</sup>, F. von Spee<sup>6</sup>, P. Stollenberg<sup>3</sup>, S. Suman<sup>10</sup>, S.K. Tandel<sup>10</sup>, J. Uusitalo<sup>9</sup>, J. Vilhena<sup>7</sup>,  
M. Williams<sup>1</sup>, G. Willmott<sup>1</sup>



